

Journal of Medicinal Chemistry

© Copyright 2004 by the American Chemical Society

Volume 47, Number 4

February 12, 2004

2003 American Chemical Society Award in Industrial Chemistry

Inhibitors of Serine Proteases as Potential Therapeutic Agents: The Road from Thrombin to Trypsin to Cathepsin G[†]

Bruce E. Maryanoff[‡]

Drug Discovery, Johnson & Johnson Pharmaceutical Research & Development, Spring House, Pennsylvania 19477-0776

Received October 1, 2003

Introduction

During my career in the pharmaceutical industry, which has spanned 30 years, the practice of drug discovery has undergone a deep-seated revolution. Around 1975, when I started as a medicinal chemist, drug discovery usually involved the synthesis of large samples (2–5 g) of new chemical compounds for broad pharmacological testing in animal models representative of a disease state of interest. In vitro testing with enzymes and receptors was very limited. Relative to the “design” of new, patent-worthy, biologically active substances, the medicinal chemist generally prepared interesting compounds with structures akin to those of known drugs, bioactive natural products, or endogenous mediators (e.g., norepinephrine, serotonin, adenosine, acetylcholine). Critical success factors were (1) efficient synthesis, especially because of the quantity of test compound required, (2) reasonably predictive in vivo pharmacological models, (3) identification and optimization of leads by in vivo testing, and (4) elimination of untoward side effects. In the decade of the 1980s, a paradigm shift occurred. Discrete molecular targets, such as receptors, enzymes, and ion channels, became available, and emphasis was placed on finding chemical entities that act on them directly with good selectivity. Also, the structures of pharmaceutically interesting macromolecular targets became increasingly abundant

from physical or computational methods. Thus, a much more “structure-based” approach to drug discovery took root. Critical success factors in this new realm still include the identification and optimization of leads, along with the avoidance of side effects. In addition, there is now a strong emphasis on controlling parameters such as drug absorption, distribution, metabolism, and excretion (ADME), especially to attain good oral bioavailability and a prolonged half-life. A diverse assemblage of technological advances, including molecular biology (cloning and expression), high-throughput synthesis (chemical libraries), high-throughput in vitro screening (lead identification), genomics, computational methods, and protein X-ray crystallography, has served to underpin this revolution. As a result, it is now rare for a medicinal chemist to prepare more than 500 mg of a test compound, and most samples are less than 100 mg. Drug discovery habits have changed to the point where pursuit of a project by the old approach would amount to a major challenge. Despite this paradigm shift and these technological advances, drug discovery still depends heavily on one key factor: good luck!

It was with considerable good fortune that I came to discover TOPAMAX topiramate under the old paradigm. Topiramate is a unique sugar sulfamate drug that is marketed worldwide for the treatment of epilepsy and is under clinical development for other therapeutic indications such as migraine headache.¹ We had set out to discover inhibitors of fructose-1,6-bisphosphatase, an important enzyme in gluconeogenesis, as potential antidiabetic agents. A synthetic intermediate derived

[†] Adapted from a lecture presented at the award symposium at the 225th National Meeting of the American Chemical Society, New Orleans, LA, March 23–27, 2003, Abstract MEDI-150.

[‡] Phone: 215-628-5530. Fax: 215-628-4985. E-mail: bmaryano@prdus.jnj.com.

from fructose, McN-4853, was screened in a panel of pharmacological assays, one of which was the maximal electroshock seizure test in mice. In an intriguing twist of fate, anticonvulsant activity was found and McN-4853 was pursued, ultimately leading to the commercial product. To be sure, this story of serendipity in pharmaceutical research is not unique.²

The combined process of drug discovery and drug development hinges on many unforeseeable factors, most of which are out of the control of any specific person. Even if the discovery and preclinical development pieces fall into place, one must still contend with the vagaries of the clinical and business development pieces. Simply put, there are huge scientific, medical, commercial, and political variables to confront, and challenges to overcome, for a product to emerge at the far end. In that respect, the necessity for good luck is further amplified. As the columnist Marilyn vos Savant has commented: "It is a wonder that drug companies can accomplish this feat at all".³

Structure-Based Drug Discovery

Molecular recognition between a drug and its biological target is fundamentally important to the expression of therapeutic efficacy. At the beginning of the 21st century, we are in a strong position to understand and utilize the critical interactions involved in such drug/macromolecule complexes. The analysis of protein structures by X-ray crystallography, NMR studies, and computer-assisted modeling has advanced to the stage of providing well-defined, three-dimensional structures in uncomplexed and ligand-complexed forms. Of course, this information can be very amenable to drug design and drug optimization.⁴ Since the intricate, specific atomic interactions attendant to ligand/receptor binding are readily accessible, at least for soluble systems, the process of "structure-based drug design" can now be widely practiced. Applications of this technique to agents that inactivate enzyme targets have proven to be particularly successful.

Structure-based drug discovery engendered a well-spring of excitement in the early 1990s, and we developed a keen interest. This approach is tantalizing because it introduces elements of rationality into the drug design process. Nevertheless, one must be cognizant of the potential perils and pitfalls, as with any technique. In this article, I will discuss aspects of our research in the area of structure-based drug discovery, which originated around 1991 with an interest in inhibitors of the serine protease thrombin. Our work then progressed to inhibitors of the serine proteases trypsin and cathepsin G.

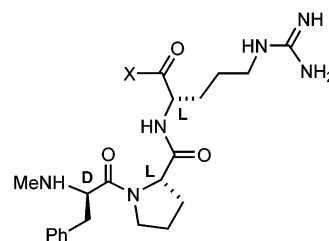
Inhibitors of Thrombin

The trypsin-like serine protease α -thrombin (EC 3.4.21.5) has received extensive attention from a structure-based perspective since the report of its first X-ray structure.⁵ Thrombin plays a central role in regulating hemostasis and thrombosis; it is crucial *inter alia* for forming blood clots and for activating platelets in response to vascular injury.⁶ In essence, thrombin protects us from bleeding to death, but it also has a down side. An excess of thrombin can lead to undesired thrombosis with accompanying death, for example, from

pulmonary embolism, myocardial infarction, or stroke. Because of this enzyme's key position in the coagulation cascade, thrombin inhibitors could be useful drugs for the treatment of thrombotic disorders,⁷ which are a serious source of mortality and morbidity in patients worldwide.

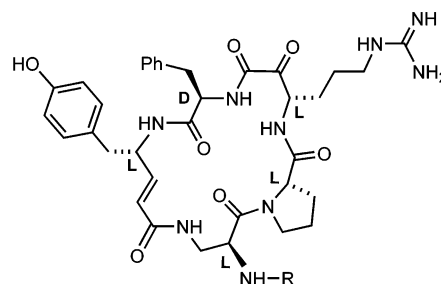
Around 1990, D-Phe-Pro-Arg-CH₂Cl (**1**; PPACK) was under examination in our laboratories for its potential as a drug development candidate.⁸ PPACK is an irreversible, active-site-directed thrombin inhibitor that operates as a "transition-state analogue" at the scissile bond area (i.e., in the region where the protease cleaves an amide bond of its protein/peptide substrate).⁹ Although PPACK was eventually set aside, this effort planted the seeds for our eventual foray into the area of thrombin inhibitors and into structure-based drug design.

Bode et al.^{5b} described the molecular structure of human α -thrombin complexed with PPACK (**1**), which depicts numerous key interactions: (1) an antiparallel β -strand between the extended backbone of the ligand and the backbone of Ser-214/Trp-215/Gly-216; (2) the guanidine occupying the S₁ specificity pocket; (3) a tetrahedral adduct formed with Ser-195; (4) alkylation of the ϵ -nitrogen of His-57 by the erstwhile chloromethyl group; (5) the methylene groups of Pro tucked into a hydrophobic S₂ cleft partly defined by residues of the 60A-I insertion loop; (6) the phenyl group of D-Phe in a hydrophobic S₃ pocket with an aromatic stacking interaction involving Trp-215.¹⁰ Additionally, this X-ray crystal structure suggests an opportunity for specific interactions with the unique 60A-I insertion loop of thrombin, especially with the side chains of Tyr-60A, Trp-60D, and Lys-60F. In the wake of this disclosure, Tulinsky, Bode, and co-workers¹¹ reported the molecular structure of human α -thrombin complexed with r-hirudin, a des-sulfate version of the famous anticoagu-



1 X = CH₂Cl (PPACK)

5 X = H (efegatran)



2a R = C(O)H (CtA)

2b R = C(O)Me (CtB)

2c R = C(O)CH₂Ph

2d R = CH₂CH₂Ph

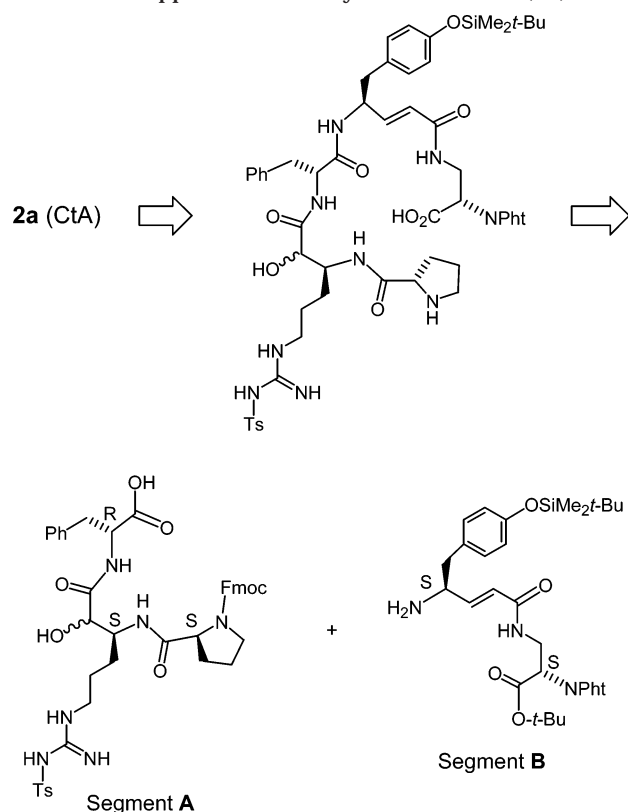
lant protein from the European medicinal leech, which depicts an elaborate collection of hydrogen bonds and electrostatic interactions. These notable achievements stimulated considerable interest in thrombin as a target for structure-based drug design.

Macrocyclic Peptides. In 1991, we initiated a project to discover novel thrombin inhibitors with the aid of the published atomic coordinates and computer-based molecular modeling. We became intrigued by the sponge-derived natural products cyclotheonamides A (**2a**, CtA) and B (**2b**, CtB),¹² which are macrocyclic peptides that inhibit thrombin, as well as some other serine proteases.^{12–14} Serine protease inhibitors based on macrocyclic peptides are rare, although such a structural motif may be found in the inhibitory loops of native protease inhibitor proteins.¹⁵ Thus, CtA struck us as a useful tool for identifying new types of interactions within the active site of thrombin and for designing novel thrombin inhibitors. In addition to its key Pro-Arg P₂–P₁ segment and P₁ electrophilic ketone, in analogy with PPACK, CtA has some important new structural features. Whereas CtA is missing the D-Phe residue at P₃ that is critical for the high thrombin affinity of the D-Phe-Pro-Arg motif,^{8a,16} it has a D-Phe in another position and a vinylogous tyrosine residue (v-Tyr), which could afford new interactions with the insertion loop or the S₁' domain of thrombin. To elucidate the mode of interaction of CtA within the active site of thrombin, we collaborated with Prof. Alexander Tulinsky (Michigan State University) to determine the structure of the thrombin/CtA/hirugen ternary complex by X-ray crystallography.¹³ A comparison of X-ray structures for the thrombin complexes of CtA and PPACK shows the disparate occupancy of the S₃ region (Figure 1). In addition to the expected features of Pro-Arg and the α -keto amide, including the γ -oxygen of Ser-195 bonded as a hemiketal (transition-state array), we found an aromatic stacking interaction between the hydroxyphenyl group of v-Tyr and Trp-60D, in the S₁' region (Figure 1). This observation lent support to the idea of capitalizing on interactions in thrombin's S₁' region with other types of molecules (vide infra).

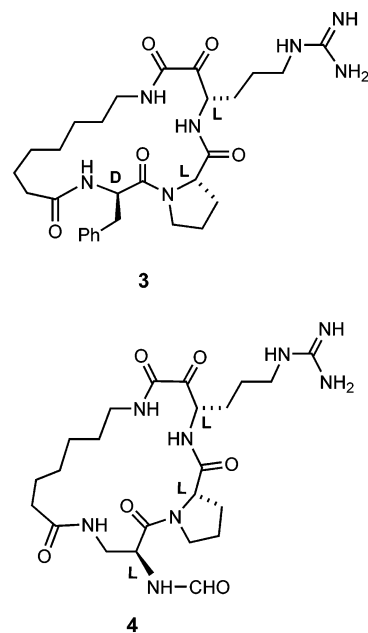
With respect to the cyclotheonamides, we completed the total synthesis of CtA and CtB;^{13,17,18} prepared and studied specific analogues to establish structure–activity relationships, which was assisted by the synthetic methodology that we developed;^{18,19} and prepared and studied novel macrocyclic D-Phe-Pro-Arg peptides as thrombin inhibitors.^{18,20} An outline of our synthesis of CtA, a convergent [3 + 2] fragment condensation protocol, is presented in Scheme 1. For details on the synthesis, the interested reader should refer to the prior literature.^{13,17,18} An important aspect of this route is the phthalimide protecting group on the pendant amino group, which can be removed at a very late stage in the synthetic sequence so that different groups could be attached. Thus, we were able to probe the hydrophobic S₃ domain of thrombin, which is not occupied by CtA but is occupied by the D-Phe-Pro-Arg motif.

Surprisingly, installation of a phenylacetyl (**2c**, $K_i = 3.1$ nM) or a 2-phenethyl (**2d**, $K_i = 1.5$ nM) substituent onto the amino group of CtA ($K_i = 4.1$ nM), to satisfy the S₃ pocket, did not result in a significant enhancement of potency.^{18,19,21} Among the CtA analogues, we

Scheme 1. Approach to the Synthesis of CtA (**2a**)



also replaced the hydroxyphenyl group with a methyl group (v-Ala) to examine the contribution to binding of the aromatic stacking interaction ($K_i = 5.3$ nM).^{18,19,21} However, since we did not obtain the anticipated 10- to 50-fold loss of thrombin inhibition, the stacking interaction alone is not especially critical. Replacement of D-Phe with D-Ala reduced thrombin inhibition by a factor of 3 ($K_i = 12$ nM), consistent with the hydrophobic nature of the S₁' subsite.^{18,19,21} Remarkably, replacement of both D-Phe and v-Tyr with their Ala equivalents caused a sharp loss of thrombin inhibition ($K_i = 230$ nM).^{18,22} This result suggests a cooperative interaction involving the two aromatic groups of the CtA ligand in



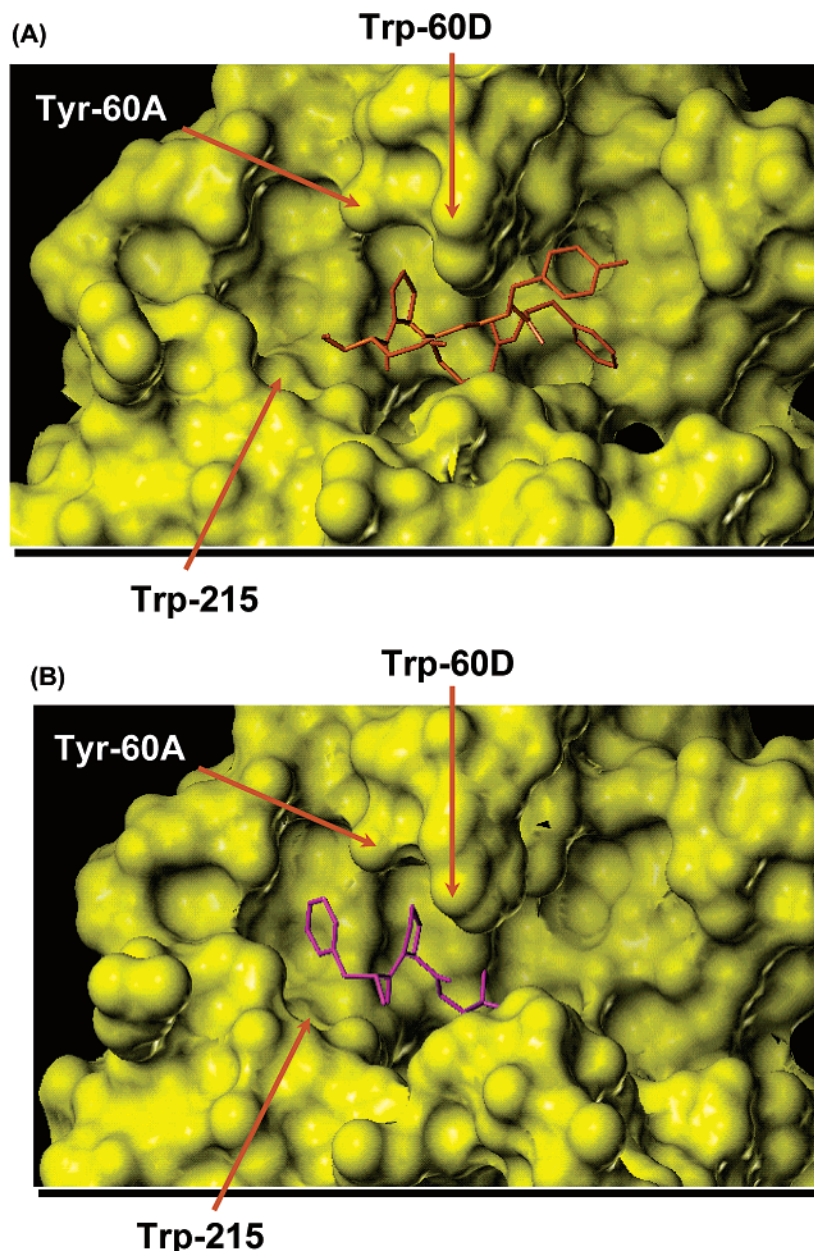


Figure 1. Comparison of the binding modes for CtA/thrombin and PPACK/thrombin. (A) Representation of the CtA/thrombin complex from X-ray crystallography¹³ displaying the active-site region. Thrombin (yellow) is shown with a Connolly surface; CtA (orange) is shown as a stick model of its non-hydrogen atoms. The S_3 hydrophobic pocket, located between residues Tyr-60A and Trp-215, is vacant. (B) Representation of the PPACK/thrombin complex from X-ray crystallography⁴ displaying the active-site region. Thrombin (yellow) is shown with a Connolly surface; PPACK (magenta) is shown as a stick model of its non-hydrogen atoms. The S_3 hydrophobic pocket is occupied by the phenyl ring of PPACK.

binding to thrombin. In our work with D-Phe-Pro-Arg macrocycles possessing oligomethylene spacers,^{18,20} we made two interesting observations relative to thrombin interactions. First, a D-Phe residue in the S_3 region was important and could not be replaced by the formamide unit of CtA, cf. **3** ($K_i = 24$ nM) and **4** ($K_i = 260$ nM).^{18,20} Second, replacement of the D-Phe and v-Tyr linkage of CtA with a hexamethylene linker, as in **4**, caused a sharp loss of affinity, consistent with what was observed for the CtA double replacement mentioned above.

Peptidoyl Heterocycles. Information gleaned from working with the cyclotheonamides indicated that one can capitalize on interactions in the S_1' subsite, especially involving the side chain of Trp-60D. Thus, we envisioned attaching a heterocycle (Het), such as 2-oxazolyl or 2-pyridyl, to the C-terminal carbonyl of a

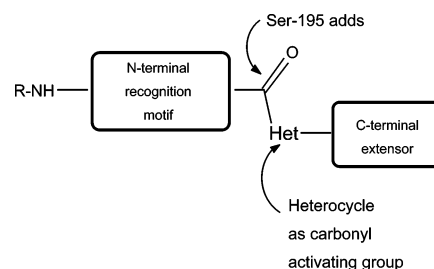
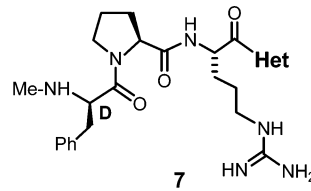
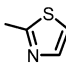
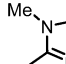
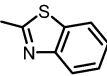
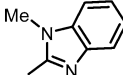
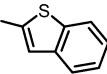
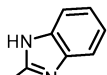
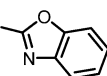
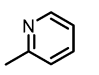
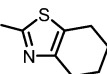
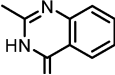


Figure 2. Strategy for the design of novel thrombin inhibitors with a heterocycle-activated ketone.

thrombin recognition motif, such as D-Phe-Pro-Arg (Figure 2).²³ These peptide-based α -keto heterocycles (also "acyl heterocycles") should be transition-state analogues with a proven thrombin binding motif, as exem-

Table 1. Data for Selected α -Ketoheterocycles


Het	K_i (nM) ^a	tryp/thr ratio ^b	compd	Het	K_i (nM) ^a	tryp/thr ratio ^b	compd
	2.1	0.6	7a		200	29	7e
	0.20	16	6a		8.1	36	7f
	2400	0.5	7b		9.6	1.2	7g
	6.2	2.1	7c		85	0.8	7h
	3.4	1.3	7d		15	0.5	7i

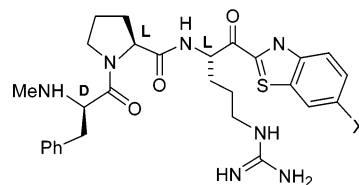
^a Value reported is generally for $N \geq 6$. ^b Thrombin selectivity in terms of (trypsin K_i)/(thrombin K_i).

plified by PPACK (**1a**) and efegatran (**5**).^{16a} The heterocycle should activate the ketone to form a reversible hemiketal adduct with the γ -oxygen of Ser-195 and provide new interactions in S_1' as well. Heterocycles can be readily modulated as to stereoelectronic properties to influence the electrophilicity of the arginine carbonyl and to serve effectively as a "C-terminal extensor" in the S_1' region. This heterocycle-activated ketone approach provided potent thrombin inhibitors, some with subnanomolar K_i values, as first reported in our preliminary publication.²⁴ In detailed articles, we have highlighted the advanced leads RWJ-50353 (**6a**), RWJ-51438 (**6b**), and RWJ-51439 (**6c**), which exhibit potent antithrombotic activity.^{25,26} The X-ray crystal structures of thrombin complexes of **6a** and **6b** have also been discussed.^{24,25,27}

Early in our studies, a seminal paper by Edwards et al. appeared with the first examples of peptide-based α -ketoheterocycles as serine protease inhibitors, in their case for elastase.²⁸ The X-ray crystal structure of Ac-Val-Pro-Val-(2-benzoxazole) complexed with porcine pancreatic elastase (PPE) depicted hemiketal formation with Ser-195 and a hydrogen-bonding interaction between the benzoxazole nitrogen and N_ϵ of His-57.²⁸ These structural features were also identified in our work with complexes of **6a**^{24,27a} and **6b**^{25,27b} with thrombin/hirugen.^{24,25,27} Since our 1996 report,²⁴ and follow-up reports by Edwards et al.,²⁹ there have been numerous papers on peptide-based α -ketoheterocycles as inhibitors of thrombin,³⁰ other serine proteases,³¹ and cysteine proteases.³²

A set of representative tripeptide α -ketoheterocycles (**6a**, **7a**–**7i**) are shown in Table 1, along with thrombin inhibition data and the selectivity for thrombin vs trypsin.^{24,25} These compounds were prepared by two main synthetic routes, one relying on a key Weinreb

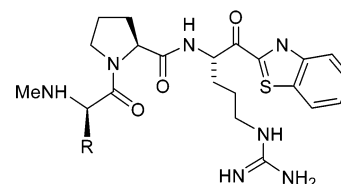
amide (Scheme 2) and the other on a key hydroxyimide (Scheme 3). For a detailed discussion of the synthesis, the interested reader should refer to our full paper.^{25,33} Benzothiazole **6a** exhibits the best thrombin inhibitory potency, with a K_i value of 0.20 ± 0.02 nM ($N = 30$). The benzo subunit enhances potency by a factor of 10 (cf. **6a** and **7a**),³⁴ and the nitrogen atom enhances potency by a factor of 12 000 (cf. **6a** and **7b**). The sulfur atom also has a significant influence because **6a** is 30 times more potent than benzoxazole **7c** and 40–50 times more potent than benzimidazoles **7f** and **7g**. Also, it is noteworthy that saturation of the benzo ring causes a 17-fold loss of potency (cf. **6a** and **6d**). Pyridine



6a X = H

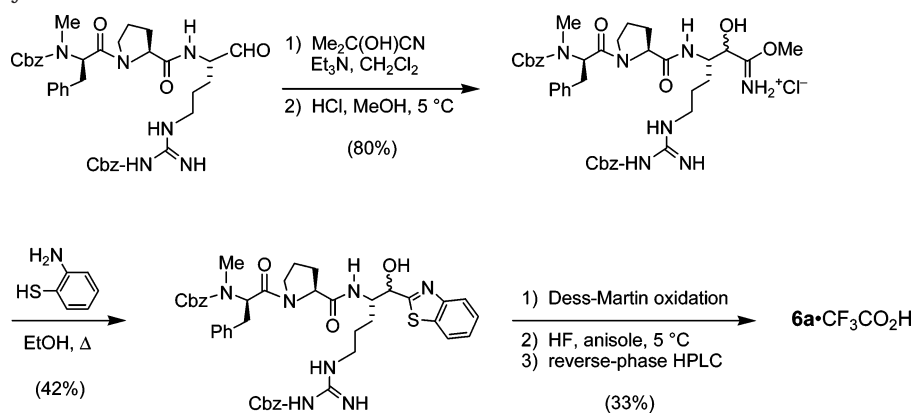
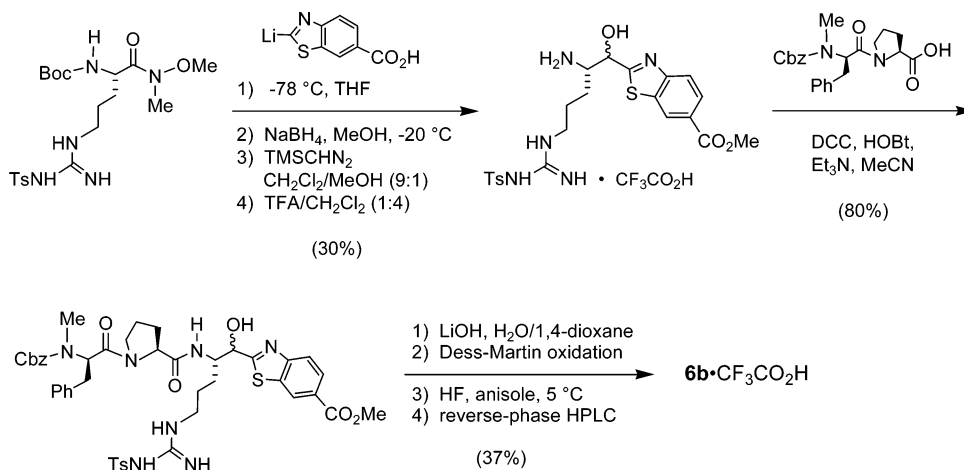
6b X = CO₂H

6c X = CO₂Me



8a R = Ph₂CH

8b R = *c*-C₆H₁₁

Scheme 2. Hydroxyimide Route to 6a**Scheme 3. Weinreb Amide Route to 6b**

6h shows a steep loss in potency, being 425-fold weaker than benzothiazole **6a** and 40-fold weaker than thiazole **7a**; quinazolinone **7i** is 50 times less potent than **6a**. Thus, certain π -rich heterocycles with a nitrogen atom and another heteroatom surrounding the attachment point are preferred.

These thrombin inhibition results are consistent with the interactions that are found in the active site of thrombin from the X-ray structures of **6a**·thrombin^{27a} and **6b**·thrombin.^{27b} The structure of **6a**·thrombin is depicted in Figure 3, and the intermolecular interactions are summarized in Figure 4. Besides the standard D-Phe-Pro-Arg interactions, the ketone forms a hemiketal with Ser-195. The benzothiazole, which resides in the S_1' subsite, displaces the side chain of Lys-60F from its normal position and into a conformationally less stable gauche arrangement. It is remarkable that **6a** is such a potent thrombin inhibitor given this effect on Lys-60F. In its favor, the benzothiazole nitrogen of **6a** hydrogen-bonds with His-57 and the benzothiazole ring is involved in an aromatic stacking interaction with Trp-60D. Additionally, through a GRID analysis, the benzothiazole sulfur atom appears to interact favorably with a hydrophobic patch on the surface of thrombin.²⁵ It is evident with **6a**·thrombin that the S_1' subsite is being occupied in a manner similar to that found with CtA·thrombin (cf. Figures 1 and 3). Compound **6a** also uses the hydrophobic S_3 region to advantage, while CtA does not.

Benzothiazole **6a** was evaluated pharmacologically as an advanced lead.^{25,26} The *in vitro* antithrombotic activ-

ity of **6a** was tested for inhibition of gel-filtered platelet (GFP) aggregation induced by α -thrombin, which provides a measure of antiplatelet activity in the absence of plasma coagulation factors and fibrinogen. An IC_{50} value of 32 ± 6 nM was obtained, which compares to an IC_{50} value of 83 ± 28 nM for efgatran (**5**). The *in vivo* antithrombotic activity of **6a** was assessed in two animal models of thrombosis: the canine arteriovenous shunt model (thrombi composed of platelets and fibrin) and the rabbit deep vein thrombosis model (thrombi composed of fibrin). In the canine thrombosis model, **6a** and efgatran (**5**) had ED_{50} values of 0.46 and 0.66 mg/kg, respectively, in reducing thrombus accumulation on a shunt-resident silk fiber (thrombogenic surface). In the rabbit thrombosis model, **6a** and efgatran had ED_{50} values of 0.29 and 0.13 mg/kg, respectively, in reducing thrombus formation.

Unfortunately, **6a** and many of its analogues elicited pronounced hypotension and electrocardiogram (ECG) effects in guinea pigs, thereby limiting their potential to advance further. Thus, representative close analogues of **6a** were prepared and evaluated for their hypotensive effects and thrombin inhibitory potency. This effort led to carboxylic acid **6b** and ester **6c**, which showed significantly diminished hypotension and ECG effects relative to **6a**.

The structure of **6b**·thrombin is largely analogous to that of **6a**·thrombin except for the carboxylate substituent on **6b** forming a salt bridge with the amino group of Lys-60F (Figure 5).^{27b} Thus, the side chain of Lys-60F is now drawn into an extended arrangement, with

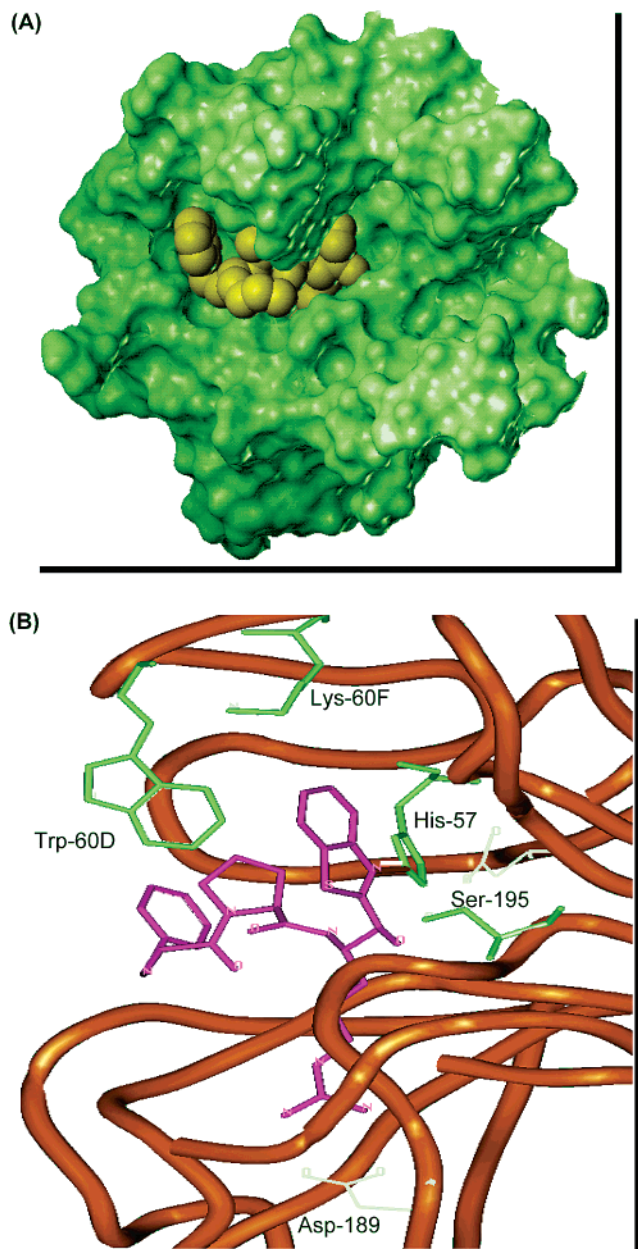


Figure 3. Representations of the **6a**·thrombin complex from X-ray crystallography,^{27a} displaying the active-site region. (A) Thrombin (green) is shown with a Connolly electron-density surface; **6a** (yellow) is shown as a space-filled model. The S_3 – S_1 regions are occupied by D-Phe-Pro-Arg, as expected, and the S_1' region is occupied by the benzothiazole group in a CtA-like manner. (B) Thrombin (orange) is shown as a ribbon diagram with certain side chains (green) installed; **6a** (magenta) is shown as a stick model of its non-hydrogen atoms. The γ -oxygen of Ser-195 is in suitable proximity to the hitherto carbonyl carbon of **6a** such that a hemiketal structure exists. The benzothiazole nitrogen is within favorable hydrogen-bonding distance relative to the ϵ -nitrogen of His-57, and the benzothiazole also participates in an aromatic stacking interaction with Trp-60D. The side chain of Lys-60F is folded up into a gauche conformation.

an anti conformation.³⁵ Steric interactions between thrombin and the carboxylate of **6b** perturb the 60A-I insertion loop relative to the loop in **6a**·thrombin (Figure 6).²⁵ Apparently, any increase in binding energy that would result from this salt-bridge formation is offset by perturbations in the enzyme due to steric interactions.

Thus, despite the strong salt-bridge interaction in **6b**·thrombin, **6b** is 10-fold less potent as a thrombin inhibitor, with a K_i value of 2.0 ± 0.9 ($N = 9$).

Benzothiazole **6b** was evaluated pharmacologically as an advanced lead.²⁵ It inhibited thrombin-induced GFP aggregation with an IC_{50} value of 41 ± 19 nM, similar to that for **6a**. In the canine arteriovenous shunt and the rabbit deep vein thrombosis models, **6b** had essentially equivalent potency to **6a**, with ED_{50} values of 0.47 and 0.30 mg/kg, respectively. Since both **6a** and **6b** exhibited low oral bioavailability ($F = 1\%$ and 3% , respectively), they did not progress further.

Our analogue studies identified some exceedingly potent thrombin inhibitors with altered P_3 substituents. For example, D-diphenylalanine **8a** and D-cyclohexylglycine **8b** displayed tight slow-binding inhibition of thrombin with K_i values of 0.00065 ± 0.0001 and 0.018 ± 0.011 nM ($N = 2$), respectively.²⁵ These compounds were also among the most potent inhibitors in our series in terms of thrombin IC_{50} values: 4.5 and 5.3 nM, respectively. Given the remarkable potency of **8a**, we prepared an analogue of it lacking the MeNH group, i.e., with a diphenylacetyl group at P_3 , and still obtained potent thrombin inhibition ($K_i = 1.1 \pm 0.3$ nM, $N = 6$).²⁵

Benzothiazole Magic. In summary, we applied structure-based drug design to discover novel, reversible, active-site-directed thrombin inhibitors, which led to potent series of macrocyclic peptides and α -keto heterocycles based on the D-Phe-Pro-Arg motif. Our observations relative to the interaction of cyclotheonamide A in the S_1' subsite of thrombin spurred us to explore the S_1' subsite with D-Phe-Pro-Arg derivatives bearing heterocyclic moieties at the C terminus. Of the various heterocycles examined, 2-benzothiazole was found to be the best (comparing K_i values) by at least an order of magnitude. Advanced lead **6a** exhibited potent activity in two animal models of thrombosis (dogs and rabbits), but it also caused hypotension and ECG effects in guinea pigs. We were able to minimize these unwanted side effects by introducing a carboxylic acid (**6b**) or a carboxylic ester (**6c**) onto the benzothiazole group. Benzothiazolecarboxylate **6b** was potent and efficacious in two animal models of thrombosis. Our structure–activity studies,²⁵ along with the X-ray structures of **6a**·thrombin and **6b**·thrombin, suggest that the improved affinity relative to aldehyde congener **1b** is primarily due to two factors: (1) the relative π -electron-withdrawing power of the benzothiazole group³⁶ and (2) the edge-to-face aromatic stacking interaction between the benzothiazole group and the indole of Trp-60D. In addition, computational analysis with GRID suggests that the benzothiazole sulfur atom may interact with a hydrophobic patch on the surface of thrombin.

The Bottom Line. Despite our success in obtaining interesting, advanced thrombin inhibitors, we were unable to pinpoint one that could be moved into pre-clinical development. In the final analysis, we were mainly hampered by low oral bioavailability of the key leads. The holy grail in this area of anticoagulant/antithrombotic therapy, starting around 1995, became an oral drug with once-a-day, or at worst twice-a-day, dosing for chronic use. That is where the greatest medical need, and the greatest business opportunity, really lies.

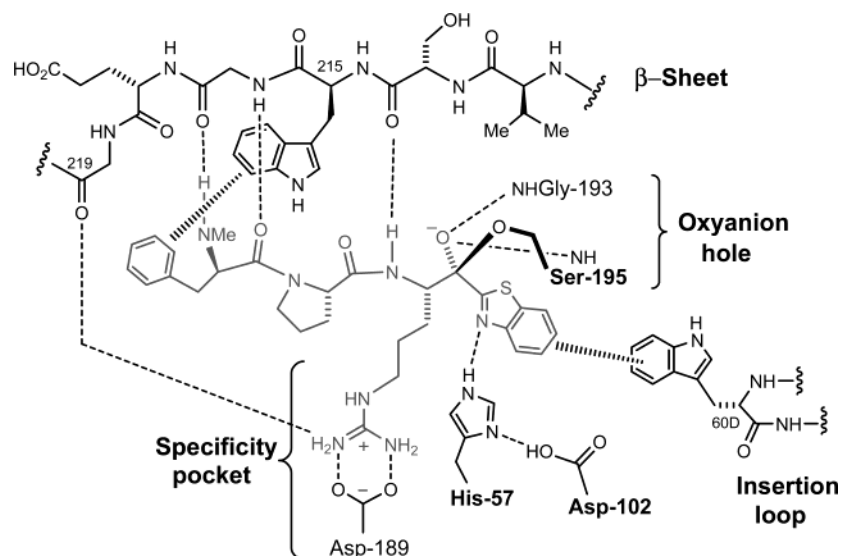


Figure 4. Schematic that summarizes the interactions between **6a** (gray) and thrombin (black) from the X-ray crystal structure.^{27a}

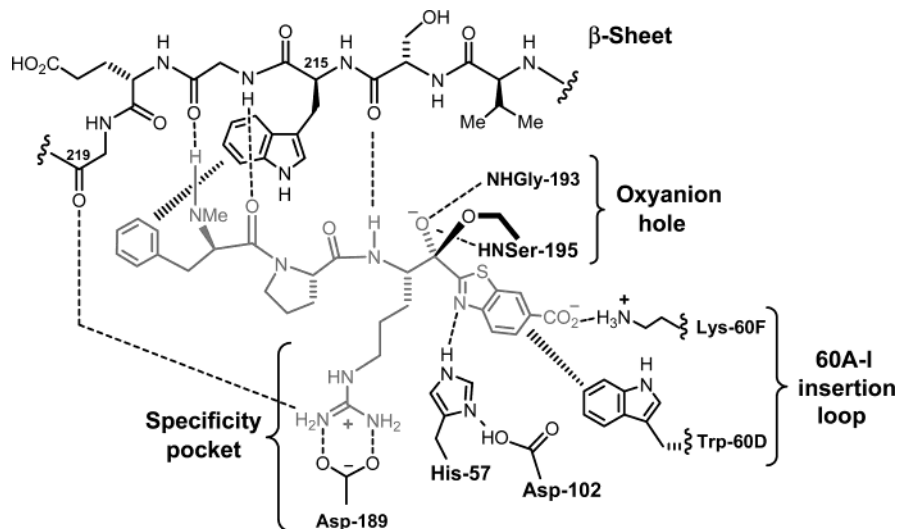


Figure 5. Schematic that summarizes the interactions between **6b** (gray) and thrombin (black) from the X-ray crystal structure.^{27b}

Transition-state analogue inhibitors (“covalent” inhibitors) have received some criticism for not being capable of yielding marketed drugs.^{7k,l} Certainly, they have been problematic in our hands, and in the hands of other researchers, because of a shortfall in pharmacokinetics. The general requirement for peptide-like structures for such inhibitors is a contributing factor. With the collective experience and clarity of hindsight now at hand, one might conclude that this approach is fraught with unacceptable perils and pitfalls. However, at this moment no orally efficacious, direct thrombin inhibitor of any type, “covalent” or “noncovalent,” has reached the marketplace. The most advanced drug candidate is the “noncovalent” inhibitor ximelagatran, which is in phase 3 clinical trials.³⁷ And ximelagatran happens to be a double prodrug of melagatran, a structural adaptation that was required to achieve the necessary druglike properties. Perhaps, there may have been more “noncovalent” than “covalent” thrombin inhibitors with suitably drugworthy characteristics, allowing the pursuit of oral clinical studies. However, the public record would indicate that neither “covalent” nor “noncovalent” thrombin inhibitors have delivered on the ultimate goal.

Inhibitors of Trypsin and Tryptase

Amidst our exploration of SAR for the α -ketoheterocycle thrombin inhibitors, we decided to test for the minimum structure to attain potent thrombin inhibition ($K_i < 10$ nM). Since the benzothiazole group conferred significant potency, we thought that it might be possible to discard the P₃ group and truncate the P₂ group. Thus, we synthesized benzothiazole **9** but found it to be a very weak inhibitor of thrombin ($K_i = 12\,300$ nM). By contrast, **9** proved to be a reasonably potent inhibitor of trypsin ($K_i = 30$ nM).³⁸ We obtained the X-ray structure of this relatively low-molecular-weight inhibitor (MW = 387.5 Da), which possesses just a capped ArgC(O)-2-benzothiazole, complexed with bovine trypsin and found that **9** occupied the active site in a manner that one would predict.³⁸ Interestingly, the benzene ring of the benzothiazole is within van der Waals distance of the Cys-42–Cys-58 disulfide bond, as part of a $\pi/S-S$ interaction, bordered by solvent molecules. Since β -tryptase has an active site cavity similar to that of trypsin, **9** was thought to have potential as a tryptase inhibitor. Our attention was drawn to tryptase as a target because this enzyme activates protease-activated

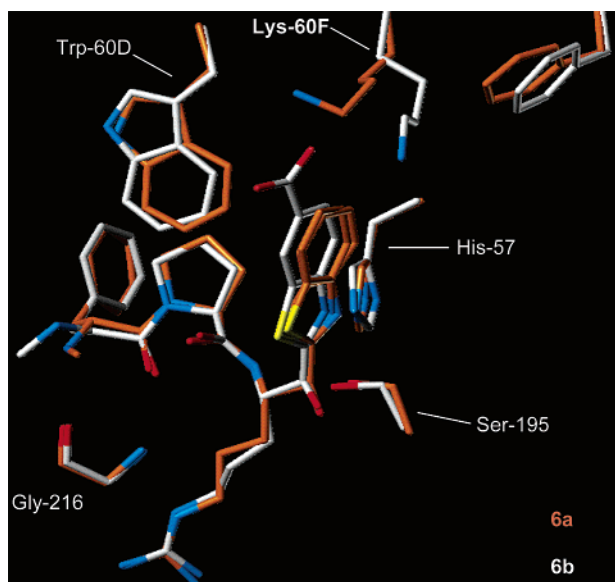


Figure 6. Comparison of features of **6a**·thrombin (orange) and **6b**·thrombin (white) in the active-site region. Inhibitors **6a** and **6b**, as well as certain amino acid side chains of thrombin, are shown as stick models of the non-hydrogen atoms; heteroatoms have standard color coding (O, red; N, blue; S, yellow).

receptor-2 (PAR-2), and we were very interested in protease-activated receptors.³⁹ Indeed, **9** turned out to inhibit tryptase with a K_i value of 88 nM, making it a very credible lead.⁴⁰

Tryptase (EC 3.4.21.59) is a homotetrameric, trypsin-like serine protease that constitutes 20–25% of the total protein of human mast cells.^{41,42} Since it is stored in a catalytically active form (rather than as a zymogen) within the secretory granules and released on stimulation, this enzyme is highly relevant to mast cell dependent inflammatory conditions.⁴¹ In fact, tryptase has been directly implicated in the pathology of asthma.⁴³ Thus, tryptase inhibitors have therapeutic potential for treating allergic or inflammatory disorders such as asthma, vascular injury, inflammatory bowel disease, and psoriasis.⁴⁴ The asthma angle looked promising to us because administration of a drug candidate directly to the lungs by inhalation seemed feasible, in which case

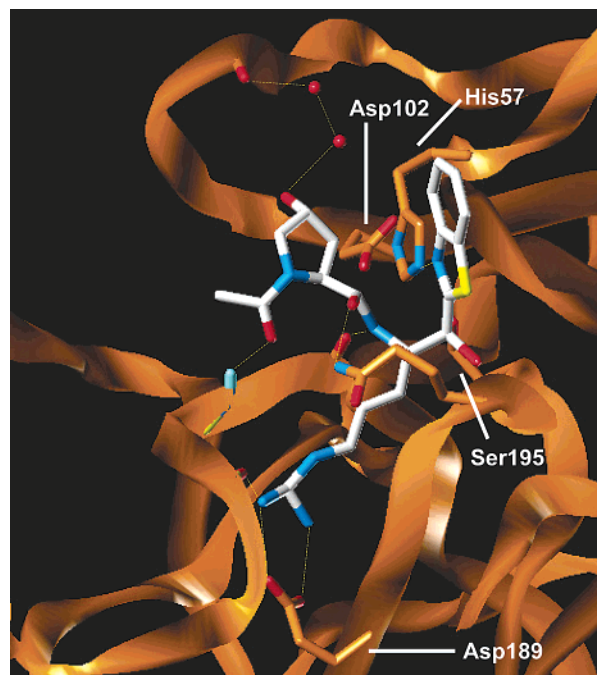
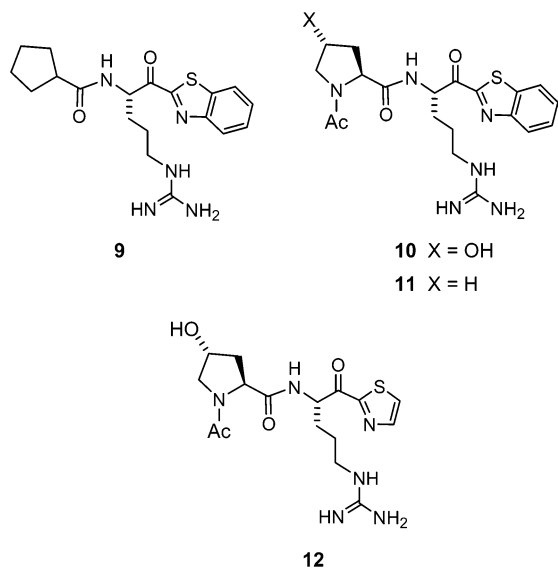


Figure 7. Representation of the **10**·trypsin complex from X-ray crystallography,⁴⁰ displaying the active-site region. View of **10** (white), shown as a stick model with the heteroatoms represented by standard color coding, bound in the active site of trypsin (orange), shown as a ribbon diagram bearing specific amino acid side chains.

the concern about oral bioavailability might be averted. Consequently, we decided to investigate analogues of **9**.⁴⁰

An early modification of the structure entailed introduction of an amide bond to interact with the β -sheet in the active site of tryptase, leading to **10** (RWJ-56423), which has the 2*S* stereochemistry.⁴⁰ This compound is a potent, reversible tryptase inhibitor with a K_i value of 10 nM.⁴⁵ Although **10** also potently inhibits trypsin ($K_i = 8.1$ nM), it is selective vs other serine proteases such as kallikrein, plasmin, thrombin, and factor Xa (selectivity of 32-, 810-, 31000-, and 5700-fold, respectively). An X-ray structure of **10** complexed with bovine trypsin shows inter alia a hemiketal involving Ser-189, a hydrogen bond between the nitrogen of the benzothiazole and $N\epsilon$ of His-57, and a hydrogen bond between the Pro secondary amide carbonyl and the side chain NH_2 of Gln-192 (Figures 7 and 8). Although a tryptase crystal structure has been published,⁴² our attempts to obtain suitable crystals of **10**·tryptase for X-ray diffraction were unsuccessful. With the X-ray coordinates for human β -tryptase,⁴² we used computational methods to obtain a three-dimensional structure of **10**·tryptase as a working model. In this complex, besides the constellation of key interactions present in the X-ray structure of **10**·trypsin, there is a new interaction between the hydroxyl of **10** and the amide side chain of Gln-98 (Figure 9). However, this interaction does not appear to be important for enzyme inhibition potency because des-hydroxyl analogue **11** has similar tryptase affinity and trypsin selectivity relative to **10**. In a comparison of the structures of **9**·trypsin and **10**·trypsin, **10** extends more deeply into the S_2 domain possibly because of hydrogen bonding between the acetyl group of **10** and Gly-216. With the high degree of homology between the

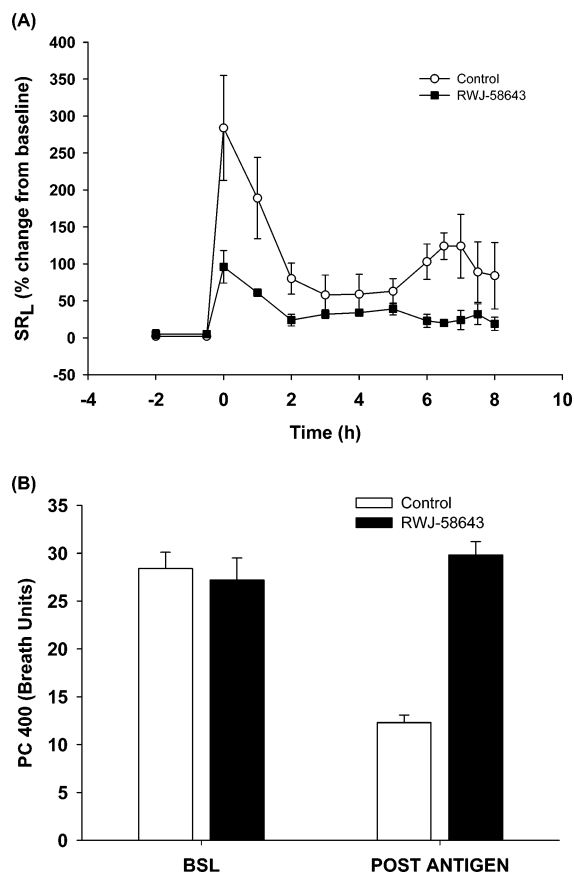


Figure 10. Administration of test compound to conscious allergic sheep by aerosol in a multiple-dosing protocol, as described in the text. (A) Increase in specific lung resistance (SR_L): (○) control animals; (■) animals treated with **6** (RWJ-58643). (B) Change in airway responsiveness at baseline (BSL) and 24 h following antigen challenge (postantigen): (open bar) control animals; (filled bar) drug-treated animals. Values are given as the mean \pm standard error for $N = 4$.

asthma.⁴⁰ The inhibitor was administered by aerosol as a total dose of 9 mg twice a day for three consecutive days and as a single, 9-mg dose on day 4, 2 h prior to antigen challenge (Figure 10). Inhaled antigen alone caused the expected airway responses under control conditions (Figure 10A). There was a mean 300% increase over baseline in specific lung resistance (SR_L; early-phase response), which returned to baseline between 2 and 6 h after challenge and increased again between 6 and 8 h after challenge to 100% over baseline (late-phase response). When these same sheep were treated with the test compound, the early response was inhibited by 70–75% and the late response was completely blocked. Twenty-four hours after antigen challenge, during carbachol administration, the sheep in the control group developed airway hyper-responsiveness as evidenced by the 2-fold decrease in the PC400, which is the dose of carbachol needed to elicit a 400% increase in SRL (Figure 10B). When these sheep were treated with test compound, this airway hyper-responsiveness was completely blocked, i.e., the postchallenge PC400 value was not different from the preantigen value.

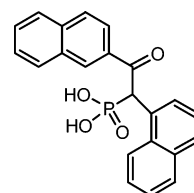
RWJ-56423 (**10**) and the diastereomeric mixture RWJ-58643 were advanced into preclinical development. The scale-up synthesis and purification of **10** as a crystalline acid addition salt was worked out. Following

favorable toxicological evaluation, **10** entered human clinical trials under an inhalation protocol.

Inhibitors of Cathepsin G and Chymase

This excursion into tryptase inhibitors drew our attention to drugs for pulmonary inflammation. Asthma and chronic obstructive pulmonary disease (COPD) are serious, unmet medical needs with a growing incidence worldwide. In this regard, we became interested in the serine protease cathepsin G (EC 3.4.21.20; Cat G), a chymotrypsin-like enzyme that is stored in the azurophilic granules of neutrophils (polymorphonuclear leukocytes) and released on degranulation.⁴⁶ Macrophages can also contain varying levels of Cat G. This protease has been implicated in a variety of pathological conditions associated mainly with inflammation.⁴⁷ For example, Cat G is involved in tissue remodeling at sites of injury via the cleavage of matrix components, including proteoglycans, collagen, fibronectin, and elastin.⁴⁸ Cathepsin G plays a role in activating protease activated receptor-4 (PAR-4), leading to platelet activation and the release of mediators that could contribute to inflammatory responses.⁴⁹ Although the endogenous protein inhibitor α 1-antichymotrypsin normally keeps Cat G in check, an imbalance occurs under inflammatory conditions, and there is a deficiency of this mediator. Thus, inhibitors of Cat G have potential for treating asthma, emphysema, reperfusion injury, psoriasis, and rheumatoid arthritis by reestablishing the balance.

Combining High-Throughput Screening and Structure-Based Design. Our initial approach to finding lead Cat G inhibitors relied on high-throughput screening of diverse compounds in the Johnson & Johnson library by using a chromogenic assay for Cat G inhibition. From our testing of nearly 250 000 compounds, we identified RWJ-48435 (**13**), which had an IC₅₀ value of $4.1 \pm 0.3 \mu\text{M}$ ($N = 6$) on follow-up evaluation. Although this compound shows just moderate potency, it is suitable for supporting an analogue study. Our interest in **13** as a prototype structure was driven by three noteworthy aspects. First, its non-peptide structure is rare among inhibitors of Cat G.^{50,51} Second, **13** is a reversible inhibitor, whereas many reported inhibitors operate through an irreversible mechanism.^{50,51} Third, the β -ketophosphonic acid group represents, to our knowledge, a novel serine protease inhibitor motif.



Given the reported 1.8 Å crystal structure of Cat G complexed with Suc-Val-Pro-Phe^P(OPh)₂,⁵¹ it is possible to apply structure-based drug design to improve on **13**. To obtain more potent Cat G inhibitors, we embarked on a two-prong approach in parallel, one involving the synthesis and testing of close analogues of **13** and the other involving X-ray diffraction of a cocrystal of **13** with

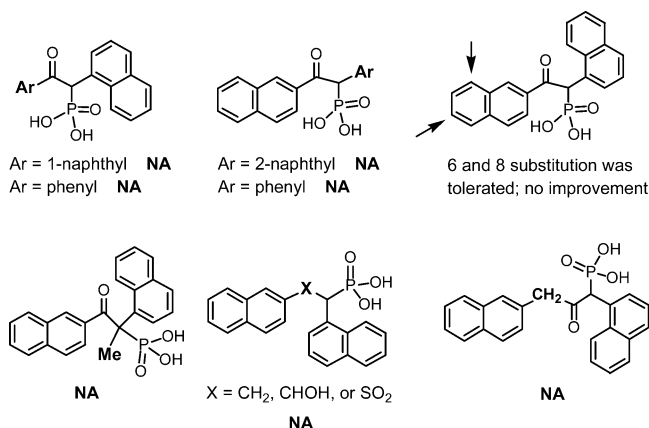


Figure 11. Some initial analogues of RWJ-48345 (**13**). NA = not active (<50% inhibition of Cat G at 100 μ M).

human Cat G. The latter approach was enabled through our collaboration with Prof. Debashish Chattopadhyay (University of Alabama–Birmingham). Of course, the crystallization experiments would be a key rate-determining step for the second prong, and there was no guarantee of success.

We synthesized numerous analogues of **13** with alterations of the aromatic rings and the ketone unit (Figure 11).⁵² Cat G inhibition was completely destroyed by replacing either naphthyl with phenyl, changing the position of substitution for each naphthyl, adding a methyl group α to phosphorus, and substituting the carbonyl with CHOH, CH₂, SO₂, or CH₂C(O). Placement of Me or OMe groups on the 2-naphthyl at the 6-position or 8-position was tolerated, but this change afforded no increase in potency.

In the meantime, we were successful in growing diffractable crystals of **13**·Cat G and in determining the X-ray structure to a resolution of 3.0 Å.⁵² Although this level of resolution is not optimal (2.5 Å or less is preferable), it is still useful for establishing the structural features of the complex. The bottom line in this case is that the X-ray structure, which is only the second X-ray structure reported for Cat G, reveals how **13** is bound within the active site and how the ligand can be optimized for greater potency.⁵²

There are two ligand/protein complexes in the asymmetric unit that are essentially the same when superimposed except for the Ile-35/Arg-41 loop in the S₁' region, which has two distinctly different conformations. One of the complexes is presented in Figure 12. The ligand in the active site of Cat G is the *R*-enantiomer of **13**, with its 2-naphthyl group in the hydrophobic S₁ specificity pocket and its 1-naphthyl group in the S₂ region (Figure 13). The distal benzene ring of the 1-naphthyl appears to participate in a π -stacking interaction with the imidazole ring of His-57 (nearly parallel planes with closest approach of 3.6 Å). The phosphonic acid is strategically deployed, with one oxygen atom hydrogen-bonded to N ϵ of His-57,⁵³ another residing in the "oxyanion hole" with hydrogen bonding to N α of Gly-193, and a third hydrogen-bonded to N ϵ of Lys-192 (Figure 14). The unenolized ketone of **13** is hydrogen-bonded to N ϵ of Lys-192. Notably, this structure reveals a vacant S₃/S₄ domain in the active-site cleft, which offers an opportunity for occupation by a suitable appendage to enhance the potency (Figures 13

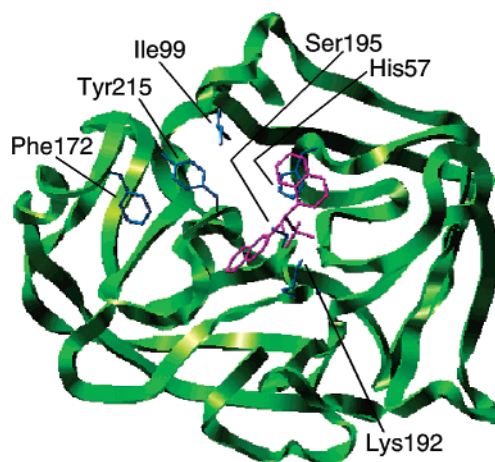


Figure 12. Structure of **13** (magenta) complexed with Cat G (green), shown as a ribbon diagram, with some key side chains (blue).⁵²

and 14B). The hydrophobic surfaces provided by the side chains of Ile-99, Phe-172, and Tyr-215 are attractive for additional ligand interactions.

We employed computer-assisted molecular modeling to test different ideas for substituting **13** with probes of the hydrophobic S₃ and S₄ subsites of Cat G. Substituents on the 1-naphthyl ring in S₂ were considered to have difficulty in reaching the S₃/S₄ area because access is impeded by Ile-99. Our analysis indicated that attachment to the 3-position of the 2-naphthyl ring would be favorable. Thus, we designed versions of **13** with a carboxamide group located on the 2-naphthyl ring to anchor a substituent that could nestle comfortably in the S₃/S₄ region, and planned to use phosphonate **14** and 2,3-naphthalic anhydride (**15**) as building blocks (Scheme 4).⁵⁴ Since our modeling gave priority to structures containing an aromatic group tethered by 6–8 Å to the 3-carboxyl, we incorporated arene-bearing amines of varying chain lengths to obtain target ligands of general type **16**.⁵²

Cat G inhibition data for carboxamide derivatives **17a–e** are given in Table 2. Analogue **17c**, with an acyclic extension, exhibits an 8-fold increase in potency over **13**, demonstrating that added hydrophobicity can enhance affinity. There was a notable 80-fold improvement over **13** with the aromatic moiety attached via a cyclic tether, as in **17d**. Presumably, the conformational constraint imparted by the piperidine ring favorably orients the phenyl portion of the ligand within Cat G's cleft. The 15-fold weaker potency of acyclic variant **17e**, compared with **17d**, supports this view. Compound **17f**, with a sizable 2-naphthyl group projecting into the hydrophobic S₃/S₄ pocket, was one of the more potent analogues ($K_i = 38$ nM). The importance of three available oxygen atoms on phosphorus was tested with **17f** by replacing one of its P–OH groups with OMe (monoester) and Me (phosphinic acid).⁵⁵ Both of these analogues resulted in a significant loss of Cat G inhibitory potency, by a factor of ca. 10.⁵⁵

For additional insight, we carried out a simulated annealing experiment (with AMBER, version 5.0) in which **17d** was docked into the active site of Cat G (Figure 15). The interactions in the S₁, S₂, and catalytic regions of this model are similar to those in the X-ray

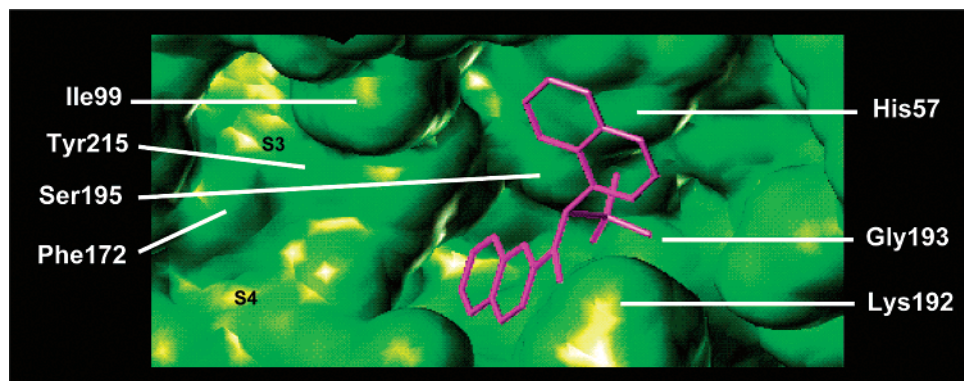


Figure 13. View of **13** (magenta), shown as a stick model, in the active site of Cat G (green), shown as a Connolly surface. The vacant S₃/S₄ pocket, on the left side, is labeled.⁵²

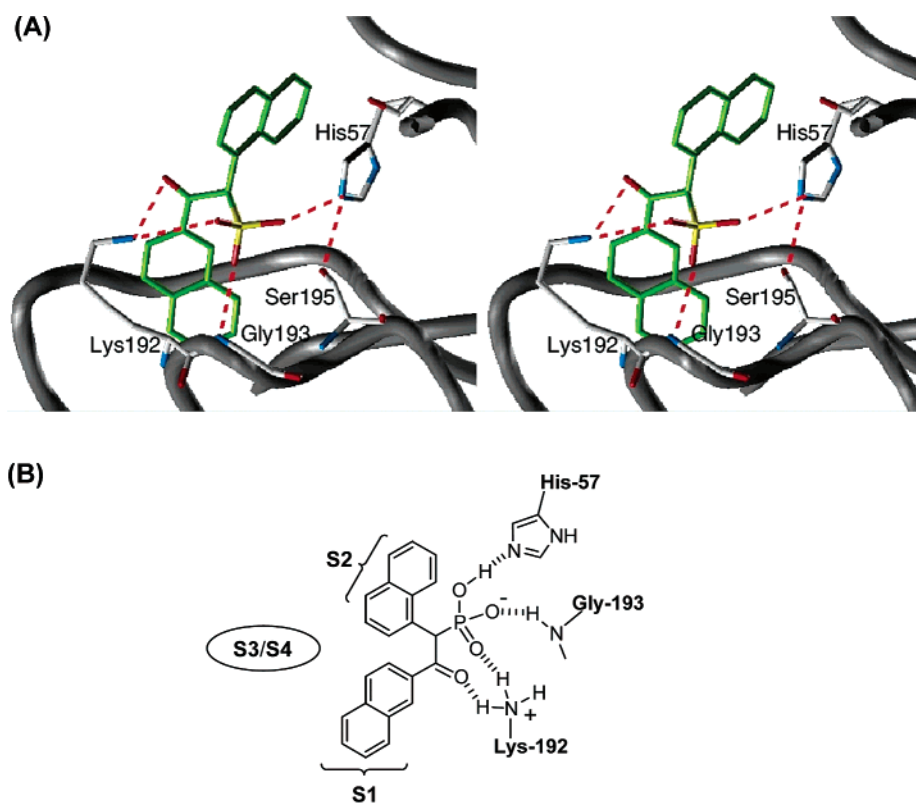
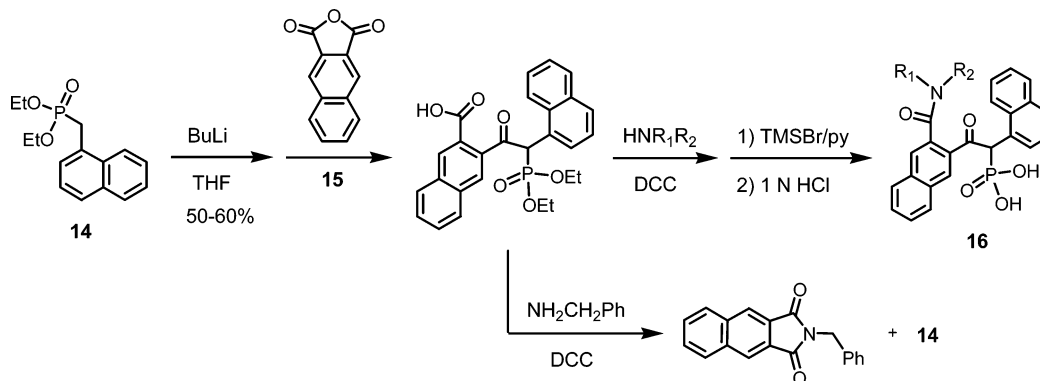


Figure 14. (A) Stereoview of the interactions of **13** (green), shown as a stick model with the heteroatoms represented by standard color coding, with Cat G.⁵² Hydrogen bonds are indicated by the broken red lines. (B) Schematic summarizing the interactions of **13** with Cat G.

Scheme 4. Synthesis of Carboxamide Analogues of **13**



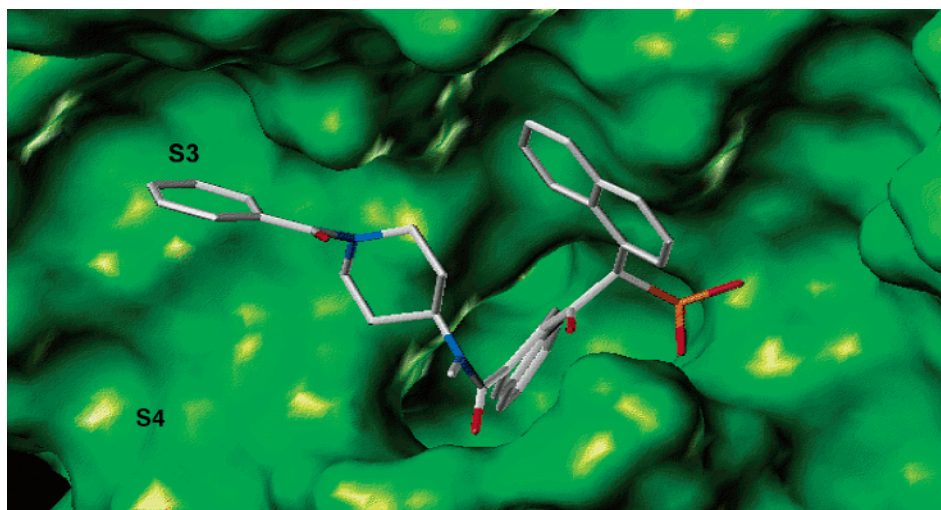
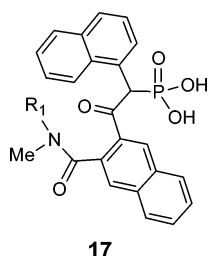




Figure 15. Model of **17d**-Cat G complex with labeling of the S₃ and S₄ domains. View of **17d** (white), shown as a stick model with the heteroatoms represented by standard color coding, bound to Cat G (green), shown as a Connolly surface.

Table 2. Cathepsin G Inhibition for Selected Carboxamide Derivatives



compd	R ₁ in 17 ^a	IC ₅₀ ± SEM, μM (N) ^b
13		4.1 ± 0.3 (6)
17a	-CH ₂ Ph	1.0 ± 0.2 (11)
17b	-CH ₂ C(O)NHCH ₂ CH ₂ Ph	1.3 ± 0.2 (9)
17c	-CH ₂ C(O)NHCH ₂ CHPh ₂	0.50 ± 0.10 (12)
17d	 NC(O)Ph	0.053 ± 0.012 (10)
17e	-(CH ₂) ₃ NHC(O)Ph	0.80 ± 0.20 (5)
17f	 NC(O)-2Np	0.038 ± 0.008 (7)

^a 2Np = 2-naphthyl. ^b N = number of experiments; SEM = standard error of the mean.

crystal structure of **13**-Cat G (Figure 13). However, the piperidine ring (chair form) positions the phenyl ring of **17d** in the S₃ pocket such that it makes hydrophobic contacts with the side chains of Phe-172, Tyr-215, and Ile-99. X-ray structural work on complexes between Cat G and inhibitor molecules is in progress.

Dual Cat G/Chymase Inhibition. Compound **17d** shows reversible, competitive inhibition with IC₅₀ and K_i values of 53 ± 12 (N = 10) and 63 ± 14 nM (N = 5), respectively. Another attribute of **17d** relates to its selectivity vs other serine proteases. It moderately inhibits chymotrypsin (K_i = 0.5 μM) and poorly inhibits (<50% inhibition at 100 μM) thrombin, factor Xa, factor IXa, plasmin, trypsin, tryptase, proteinase 3, and human leukocyte elastase.⁵² Surprisingly, **17d** is a potent

inhibitor of chymase with an IC₅₀ value of 17 ± 5 (N = 3); thus, it is a dual inhibitor of Cat G and chymase.

Chymase (EC 3.4.21.39) is a chymotrypsin-like serine protease that is present mainly in the secretory granules of mast cells and is released on degranulation.⁵⁶ Chymase, like Cat G, cleaves extracellular matrix components. Moreover, this enzyme plays a role in the initiation of inflammatory responses that affect the formation of chemokines and possibly cytokines, which then stimulate the infiltration of secondary inflammatory cells, such as neutrophils. In a different vein, chymase can convert angiotensin-I to angiotensin-II to stimulate vascular permeability. Both chymase and Cat G are postulated to have effects on tissue remodeling in the blood vessel wall, heart, and lungs. α₁-Antichymotrypsin and α₁-proteinase inhibitor are endogenous protein inhibitors that normally keep chymase in check. However, under inflammatory conditions an imbalance can occur between the levels of these mediators and chymase, with there being a deficiency of the inhibitors. Thus, synthetic inhibitors of chymase have potential for treating inflammatory disorders such as asthma, reperfusion injury, and psoriasis.^{57,58}

It appears that a dual inhibitor of Cat G and chymase would have significant potential as an antiinflammatory agent, and we set out to demonstrate that fact with suitable pharmacological models. An excellent response was found for **17f** in the standard sheep model of asthma, as described in our published patent.⁵⁵ As shown in Figure 16, the early-phase asthmatic response is significantly blunted and the late-phase asthmatic response is completely ablated. Also, we observed interesting antiinflammatory activity for a dual inhibitor in a rat peritonitis model. Glycogen-induced peritonitis was inhibited as determined by a reduction in neutrophil influx into the peritoneal fluid and a reduction in the levels of the neutrophil chemokines IL-1α, IL-1β, and MCP-1.⁵⁹ Studies in other animal models of inflammation have also delivered positive findings.⁵⁹ Such results reflect favorably on the potential of a dual Cat G/chymase inhibitor for the treatment of inflammatory disorders in humans.

Novel Serine Protease Inhibitor Motif. There are known serine protease inhibitors that possess phospho-

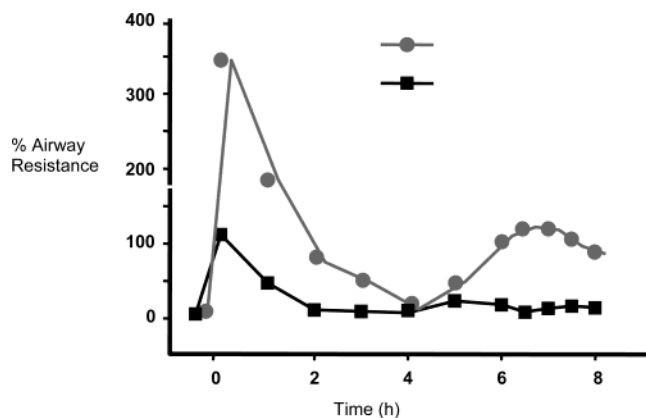


Figure 16. Response of **17f** in the allergen-sensitized sheep model of asthma.⁵⁵ Protocol: 0.1 mg/kg of **17f** was administered by aerosol twice daily for 3 days and then at 0.5 h before day 4, when the allergen *Ascaris suum* was delivered.

nate or phosphinate groups, which can occupy the active site in the vicinity of the catalytic residues Ser-195 and His-57.^{51,60–62} However, such inhibitors have generally been P-ester forms, especially diphenyl phosphonates, and they operate by slow-tight or irreversible binding.^{51,60,61} Indeed, the formation of a covalent bond with O γ of Ser-195 has been confirmed by three different X-ray studies.^{51,61e,g} In reports concerning serine protease inhibitors bearing a free phosphonic or phosphinic acid end-group, the compounds of interest also have an acylamino group on the carbon α to phosphorus.^{62a–c,63} The known phosphonate and phosphinate ester inhibitors also usually possess this structural element.⁶⁰ In this regard, such inhibitors can be viewed as surrogates for, or mimics of, α -amino acid residues in a peptide fragment. Our case is quite different. We have identified non-peptide inhibitors with a novel β -ketophosphonic acid core structure, which represents a new serine protease inhibitor motif. The phosphonic acid supplies three oxygen atoms in the binding to the enzyme, and the ketone β to phosphorus also plays an important role in binding (Figure 14). This β -ketophosphonic acid core structure has the potential for wider applicability in the design of serine protease inhibitors. One can imagine potent inhibitors for other types of serine proteases that incorporate structural features for favorable interactions within the relevant S₁–S₃ subsites.

Epilogue

Over the past 15 years or so, structure-based drug discovery has taken over the practice of medicinal chemistry by a storm. We began our efforts in 1991, when the technique was still in its inchoative period, with the design of novel inhibitors of thrombin. Subsequently, we extended our work with serine proteases to inhibitors of tryptase/trypsin and cathepsin G/chymase. Potent enzyme inhibitors with significant efficacy in preclinical models of disease were obtained in each class, and at least one new chemical entity was advanced into human clinical study. In the case of Cat G, we capitalized on the marriage of high-throughput screening and structure-based drug design to convert a lead with modest potency into an inhibitor with a 100-fold potency improvement. Thus, we reached a reasonable potency level to allow for meaningful pharmacological studies. In the process, we were fortunate to

discover even better potency for the inhibition of chymase, giving rise to a novel family of dual Cat G/chymase inhibitors. This odyssey has been very intellectually satisfying. However, looking back, it is clear that successful structure-based drug discovery not only requires considerable intellectual input but also requires considerable insight and intuition, and good luck. These qualities are basically no different from those needed for the success of any type of modern medicinal-chemistry-driven project.

Acknowledgment. I am very honored to receive the prestigious 2003 ACS Award in Industrial Chemistry, and I thank the ACS Division of Business Development and Management for its sponsorship. I am indebted to many excellent collaborators who have participated in the serine protease inhibitor projects over the years and whose names appear in many of the cited references. In particular, I want to recognize the key scientific leaders in the company who collaborated with me on this effort: Harold R. Almond, Jr., Patricia Andrade-Gordon, Michael J. Costanzo, Bruce P. Damiano, Lawrence de Garavilla, Edward C. Giardino, and Michael N. Greco. I am very grateful to Alexander Tulinsky for his guidance in the X-ray crystallography of thrombin and for his consultations on structure-based drug design and to Debashish Chattopadhyay for his X-ray crystallography work on trypsin and cathepsin G. I thank my wife Cyndie for her excellent support during my career; it has been a great positive influence. Finally, I want to acknowledge the support from Johnson & Johnson over the course of my 30-year career.

Biography

Bruce E. Maryanoff. After earning B.S. (1969) and Ph.D. (1972) degrees from Drexel University, Dr. Maryanoff conducted postdoctoral studies at Princeton University. He joined McNeil Laboratories, a Johnson & Johnson company, in 1974 and advanced to Distinguished Research Fellow, the highest scientific position. From 1976 to 1992, he principally worked on drugs for central nervous system disorders, whence he discovered TOPAMAX topiramate, which is marketed worldwide for treating epilepsy and is under development for migraine. In 1992, he moved into cardiovascular research and presently leads the Vascular Research Team. Dr. Maryanoff has published 200 scientific papers, is an inventor on 65 U.S. patents (issued or pending), and has received two national awards from the American Chemical Society (Heroes of Chemistry Award in 2000; Award in Industrial Chemistry in 2003).

References

- (1) (a) For information on TOPAMAX topiramate, refer to www.topamax.com. (b) Also, see the following: Maryanoff, B. E.; Nortey, S. O.; Gardocki, J. F.; Shank, R. P.; Dodgson, S. P. Anticonvulsant O-alkyl sulfamates. 2,3:4,5-Bis-O-1-methylethylidene- β -D-fructopyranose sulfamate and related compounds. *J. Med. Chem.* **1987**, *30*, 880–887. Shank, R. P.; Gardocki, J. F.; Vaught, J. L.; Davis, C. B.; Schupsky, J. J.; Raffa, R. B.; Dodgson, S. J.; Nortey, S. O.; Maryanoff, B. E. Topiramate: preclinical evaluation of a structurally novel anticonvulsant. *Epilepsia* **1994**, *35*, 450–460. Maryanoff, B. E.; Costanzo, M. J.; Nortey, S. O.; Greco, M. N.; Shank, R. P.; Schupsky, J. J.; Ortegón, M. P.; Vaught, J. L. Structure-activity studies on anticonvulsant sugar sulfamates related to topiramate. Enhanced potency with cyclic sulfate derivatives. *J. Med. Chem.* **1998**, *41*, 1315–1343. Shank, R. P.; Gardocki, J. F.; Streeter, A. J.; Maryanoff, B. E. An overview of the preclinical aspects of topiramate: pharmacology, pharmacokinetics, and mechanism of action. *Epilepsia* **2000**, *41* (Suppl. 1), S3–S9. Garnett, W. R. Clinical pharmacology of topiramate: a review. *Epilepsia* **2000**, *41* (Suppl. 1), S61–S65. Ben-Menachem, E. The clinical efficacy of topiramate in the treatment

- of epilepsy. *Rev. Contemp. Pharmacother.* **1999**, *10*, 163–184.
- Tomson, T. Newer antiepileptic drugs and recent advances in drug therapy of epilepsy. *Curr. Sci.* **2002**, *82*, 698–706.
- Faught, E. Clinical studies of topiramate. *Drugs Today* **1999**, *35*, 49–57.
- Michelucci, R.; Passarelli, D.; Riguzzi, P.; Volpi, L.; Tassinari, C. A. The preclinical and therapeutic activity of the novel anticonvulsant topiramate. *CNS Drug Rev.* **1998**, *4*, 165–186.
- (2) Meyer, P. Discovering new drugs: the legacy of the past, present approaches, and hopes for the future. In *The Practice of Medicinal Chemistry*; Wermuth, C. G., Ed.; Academic Press: San Diego, CA, 1996; pp 11–24.
- Wolff, M. E., Ed. *Burger's Medicinal Chemistry and Drug Discovery*, 5th ed.; Wiley: New York, 1995; Vol. 1.
- Sneader, W. Chronology of drug introductions. In *Comprehensive Medicinal Chemistry*; Hansch, C., Sammes, P. G., Taylor, J. B., Eds.; Pergamon Press: Oxford, 1990; pp 8–80.
- Sneader, W. *Drug Prototypes and Their Exploitation*; Wiley: Chichester, U.K., 1996.
- (3) vos Savant, M. Ask Marilyn. *Parade* **2003**, February 2.
- (4) Some reviews pertinent to structure-based drug design and discovery: (a) Appelt, K.; Bacquet, R. J.; Bartlett, C. A.; Booth, C. L.; Freer, S. T.; Fuhry, M. A.; Gehring, M. R.; Herrmann, S. M.; Howland, E. F.; Janson, C. A.; et al. Design of enzyme inhibitors using iterative protein crystallographic analysis. *J. Med. Chem.* **1991**, *34*, 1925–1934. (b) Greer, J.; Erickson, J. W.; Baldwin, J. J.; Varney, M. D. Application of the three-dimensional structures of protein target molecules in structure-based drug design. *J. Med. Chem.* **1994**, *37*, 1035–1054. (c) Reickson, J. W.; Fesik, S. W. Macromolecular X-ray crystallography and NMR as tools for structure-based drug design. *Annu. Rev. Med. Chem.* **1992**, *27*, 217–289. (d) McDowell, R. S.; Artis, D. R. Structure-based design from flexible ligands. *J. Med. Chem.* **1995**, *30*, 265–274. (e) Kuntz, I. D.; Meng, E. C.; Shoichet, B. K. Structure-based molecular design. *Acc. Chem. Res.* **1994**, *27*, 117–123. (f) Bode, W.; Huber, R. Structural basis of the endoproteinase–protein inhibitor interaction. *Biochim. Biophys. Acta* **2000**, *1477*, 241–252.
- (5) (a) The catalytic machinery in the active site of thrombin and other serine proteases comprises the catalytic triad His-57, Asp-104, and Ser-195 (chymotrypsinogen numbering system^{5b}). (b) Bode, W.; Mayr, I.; Baumann, U.; Huber, R.; Stone, S. R.; Hofsteenge, J. The refined 1.9 Å crystal structure of α -thrombin: interaction with D-Phe-Pro-Arg chloromethylketone and significance of the Tyr-Pro-Pro-Trp insertion segment. *EMBO J.* **1989**, *8*, 3467–3475. Bode, W.; Turk, D.; Karshikov, A. The refined 1.9 Å X-ray crystal structure of D-Phe-Pro-Arg chloromethylketone-inhibited human α -thrombin: structure analysis, overall structure, electrostatic properties, detailed active-site geometry, and structure–function relationships. *Protein Sci.* **1992**, *1*, 426–471.
- (6) (a) Berliner, L. J., Ed. *Thrombin: Structure and Function*; Plenum Press: New York, 1992. (b) Davie, E. W.; Fugikawa, K.; Kisiel, W. The coagulation cascade: initiation, maintenance, and regulation. *Biochemistry* **1991**, *30*, 10363–10370.
- (7) For reviews on thrombin inhibitors, see the following. (a) Maffrand, J. P. Direct thrombin inhibitors. *Nouv. Rev. Fr. Hematol.* **1992**, *34*, 405–419. (b) Talbot, M. D.; Butler, K. D. Potential clinical uses of thrombin inhibitors. *Drug News Perspect.* **1990**, *3*, 357–363. (c) Das, J.; Kimball, S. D. Thrombin active site inhibitors. *Bioorg. Med. Chem.* **1995**, *3*, 999–1007. (d) Scarborough, R. M. Anticoagulant strategies targeting thrombin and factor Xa. *Annu. Rev. Med. Chem.* **1995**, *30*, 71–80. (e) Kimball, S. D. Thrombin active site inhibitors. *Curr. Pharm. Des.* **1995**, *1*, 441–468. (f) Fareed, J.; Callas, D. D. Pharmacological aspects of thrombin inhibitors: a developmental perspective. *Vessels* **1995**, *1*, 15–24. (g) Lefkovits, J.; Topol, E. J. Direct thrombin inhibitors in cardiovascular medicine. *Circulation* **1994**, *90*, 1522–1536. (h) Betschmann, P.; Lerner, C.; Sahli, S.; Obst, U.; Diederich, F. Molecular recognition with biological receptors: structure-based design of thrombin inhibitors. *Chimia* **2000**, *54*, 633–639. (i) Menear, K. Direct thrombin inhibitors: Current status and future prospects. *Expert Opin. Invest. Drugs* **1999**, *8*, 1373–1384. (j) Ripka, W. C.; Vlasuk, G. P. Antithrombotics/serine proteases. *Annu. Rev. Med. Chem.* **1997**, *32*, 71–89. (k) Sanderson, P. E. J. Small, noncovalent serine protease inhibitors. *Med. Res. Rev.* **1999**, *19*, 179–197. (l) Kimball, S. D. Challenges in the development of orally bioavailable thrombin active site inhibitors. *Blood Coagulation Fibrinolysis* **1995**, *6*, 511–519.
- (8) (a) Kettner, C.; Shaw, E. D-Phe-Pro-ArgCH₂Cl—a selective affinity label for thrombin. *Thromb. Res.* **1979**, *14*, 969–973.
- Hauptmann, J.; Markwardt, F. Studies on the anticoagulant and antithrombotic action of an irreversible thrombin inhibitor. *Thromb. Res.* **1980**, *20*, 347–351. (b) This product opportunity arose from a relationship between Johnson & Johnson and The Scripps Research Institute. For background on the antithrombotic action of PPACK, see the following. Hanson, S. R.; Harker, L. A. Interruption of acute platelet-dependent thrombosis by the synthetic antithrombin D-phenylalanyl-L-prolyl-L-arginyl chloromethyl ketone. *Proc. Natl. Acad. Sci. U.S.A.* **1988**, *85*, 3184–3188.
- Lumsden, A. B.; Kelly, A. B.; Schneider, P. A.; Krupski, W. C.; Dodson, T.; Hanson, S. R.; Harker, L. A. Lasting safe interruption of endarterectomy thrombosis by transiently infused antithrombin peptide D-Phe-Pro-ArgCH₂Cl in baboons. *Blood* **1993**, *81*, 1762–1770.
- (9) (a) The term “transition-state analogue” is used somewhat loosely here. “Reaction coordinate analogue” has been proposed as a more precise term for a reversible enzyme inhibitor involving an electrophilic center that covalently attaches to a group in the enzyme active site.^{9b} (b) Christianson, D. W.; Lipscomb, W. N. Carboxypeptidase A. *Acc. Chem. Res.* **1989**, *22*, 62–69.
- (10) The nomenclature system of Schechter and Berger, which designates the amino acid residues flanking the scissile bond as “...P₂–P₁–P₁'–P₂'...” (and the corresponding subsites as “...S₂–S₁–S₁'–S₂'...”), is used throughout this paper. Schechter, I.; Berger, A. On the size of the active site in proteases. I. Papain. *Biochem. Biophys. Res. Commun.* **1967**, *27*, 157–162.
- (11) Rydel, T. J.; Ravichandran, K. G.; Tulinsky, A.; Bode, W.; Huber, R.; Roitsch, C.; Fenton, J. W., II. The structure of a complex of recombinant hirudin and human α -thrombin. *Science* **1990**, *249*, 277–280.
- (12) Fusetani, N.; Matsunaga, S.; Matsumoto, H.; Takebayashi, Y. Bioactive marine metabolites. 33. Cyclotheonamides, potent thrombin inhibitors, from a marine sponge *Theonella* sp. *J. Am. Chem. Soc.* **1990**, *112*, 7053–7054.
- (13) Maryanoff, B. E.; Qiu, X.; Padmanabhan, K. P.; Tulinsky, A.; Almond, H. R., Jr.; Andrade-Gordon, P.; Greco, M. N.; Kauffman, J. A.; Nicolaou, K. C.; Liu, A.; Brungs, P. H.; Fusetani, N. Molecular basis for the inhibition of human α -thrombin by the macrocyclic peptide cyclotheonamide A. *Proc. Natl. Acad. Sci. U.S.A.* **1993**, *90*, 8048–8052.
- (14) Lewis, S. D.; Ng, A. S.; Baldwin, J. J.; Fusetani, N.; Naylor, A. M.; Shafer, J. A. Inhibition of thrombin and other trypsin-like serine proteases by cyclotheonamide A. *Thromb. Res.* **1993**, *70*, 173–190.
- (15) Gettins, P. G. W. Serpin structure, mechanism, and function. *Chem. Rev.* **2002**, *102*, 4751–4803.
- Ye, S.; Goldsmith, E. J. Serpins and other covalent protease inhibitors. *Curr. Opin. Struct. Biol.* **2001**, *11*, 740–745.
- Otlewski, J.; Krowarsch, D.; Apostoluk, W. Protein inhibitors of serine proteases. *Acta Biochim. Pol.* **1999**, *46*, 531–565.
- McBride, J. D.; Watson, E. M.; Brauer, A. B. E.; Jaulent, A. M.; Leatherbarrow, R. J. Peptide mimics of the Bowman–Birk inhibitor reactive site loop. *Biopolymers* **2002**, *66*, 79–92.
- McBride, J. D.; Leatherbarrow, R. J. Synthetic peptide mimics of the Bowman–Birk inhibitor protein. *Curr. Med. Chem.* **2001**, *8*, 909–917.
- (16) (a) Bajusz, S.; Szell, E.; Bagdy, D.; Barabas, E.; Horvath, G.; Dioszegi, M.; Fittler, Z.; Szabo, G.; Juhasz, A.; Tomori, E.; Szilagyi, G. Highly active and selective anticoagulants: D-Phe-Pro-Arg-H, a free tripeptide aldehyde prone to spontaneous inactivation, and its stable N-methyl derivative, D-MePhe-Pro-Arg-H. *J. Med. Chem.* **1990**, *33*, 1729–1735. (b) Tomori, E.; Szell, E.; Barabas, E. High-performance liquid chromatography of a new tripeptide aldehyde (GYKI-14166), correlation between the structure and activity. *Chromatographia* **1984**, 437–442. (c) Shuman, R. T.; Rothenberger, R. B.; Campbell, C. S.; Smith, G. F.; Gifford-Moore, D. S.; Gesellchen, P. D. Highly selective tripeptide thrombin inhibitors. *J. Med. Chem.* **1993**, *36*, 314–319.
- (17) Maryanoff, B. E.; Greco, M. N.; Zhang, H.-C.; Andrade-Gordon, P.; Kauffman, J. A.; Nicolaou, K. C.; Liu, A.; Brungs, P. H. Macrocyclic peptide inhibitors of serine proteases. Convergent synthesis of cyclotheonamides A and B via a late-stage primary amine intermediate. Study of thrombin inhibition under diverse conditions. *J. Am. Chem. Soc.* **1995**, *117*, 1225–1239.
- (18) Greco, M. N.; Maryanoff, B. E. Macrocyclic inhibitors of serine proteases. *Adv. Amino Acid Mimetics Peptidomimetics* **1997**, *1*, 41–76.
- (19) Maryanoff, B. E.; Zhang, H.-C.; Greco, M. N.; Glover, K. A.; Kauffman, J. A.; Andrade-Gordon, P. Cyclotheonamide derivatives: synthesis and thrombin inhibition. Exploration of specific structure–function issues. *Bioorg. Med. Chem.* **1995**, *3*, 1025–1038.
- (20) Greco, M. N.; Powell, E. T.; Hecker, L. R.; Andrade-Gordon, P.; Kauffman, J. A.; Lewis, J. M.; Ganesh, V.; Tulinsky, A.; Maryanoff, B. E. Novel thrombin inhibitors that are based on a macrocyclic tripeptide motif. *Bioorg. Med. Chem. Lett.* **1996**, *6*, 2947–2952.
- (21) Conditions were biased to slow-binding (rather than Michaelis–Menten) kinetics.
- (22) Conditions were biased to Michaelis–Menten kinetics. We observed no slow-binding behavior for this double-replacement CtA analogue. Consequently, the Michaelis–Menten K_i value of 230 nM is being compared to the slow-binding K_i values for the other analogues.

- (23) An *N*-methyl group was incorporated in the D-Phe-Pro-Arg compounds to avoid possible imine formation between a primary amino terminus and the activated ketone, which could lead to self-condensation or decomposition.^{16a}
- (24) Costanzo, M. J.; Maryanoff, B. E.; Hecker, L. R.; Schott, M. R.; Yabut, S. C.; Zhang, H.-C.; Andrade-Gordon, P.; Kauffman, J. A.; Lewis, J. M.; Krishnan, R.; Tulinsky, A. Potent thrombin inhibitors that probe the S₁' subsite: tripeptide transition state analogs based on a heterocycle-activated carbonyl group. *J. Med. Chem.* **1996**, *39*, 3039–3043.
- (25) Costanzo, M. J.; Almond, H. R., Jr.; Hecker, L. R.; Schott, M. R.; Yabut, S. C.; Zhang, H.-C.; Andrade-Gordon, P.; Corcoran, T. W.; Giardino, E. C.; Kauffman, J. A.; Lewis, J. M.; de Garavilla, L.; Haertlein, B.; Maryanoff, B. E. In-depth study of tripeptide ketoheterocycles as inhibitors of thrombin. Effective utilization of the S₁' subsite and its implications to structure-based drug design. *J. Med. Chem.*, in press.
- (26) Giardino, E. C.; Costanzo, M. J.; Kauffman, J. A.; Li, Q. S.; Maryanoff, B. E.; Andrade-Gordon, P. Antithrombotic properties of RWJ-50353, a potent and novel thrombin inhibitor. *Thromb. Res.* **2000**, *98*, 83–93.
- (27) (a) Matthews, J. H.; Krishnan, R.; Costanzo, M. J.; Maryanoff, B. E.; Tulinsky, A. Crystal structures of thrombin with thiazole-containing inhibitors: probes of the S₁' binding site. *Biophys. J.* **1996**, *71*, 2830–2839. (b) Recacha, R.; Costanzo, M. J.; Maryanoff, B. E.; Carson, M.; DeLucas, L. J.; Chattopadhyay, D. Crystal structure of human α -thrombin complexed with RWJ-51438 at 1.7 Å: unusual perturbation of the 60A-60I insertion loop. *Acta Crystallogr., Sect. D: Biol. Crystallogr.* **2000**, *D56*, 1395–1400.
- (28) Edwards, P. D.; Meyer, E. F., Jr.; Vijayalakshmi, J.; Tuthill, P. A.; Andisik, D. A.; Gomes, B.; Strimpler, A. Design, synthesis, and kinetic evaluation of a unique class of elastase inhibitors, the peptidyl α -ketobenzoxazoles, and the X-ray crystal structure of the covalent complex between porcine pancreatic elastase and Ac-Ala-Pro-Val-2-benzoxazole. *J. Am. Chem. Soc.* **1992**, *114*, 1854–1863.
- (29) Edwards, P. D.; Wolanin, D. J.; Andisik, D. W.; Davis, M. W. Peptidyl α -ketoheterocyclic inhibitors of human neutrophil elastase. 2. Effect of varying the heterocyclic ring on in vitro potency. *J. Med. Chem.* **1995**, *38*, 76–85. Edwards, P. D.; Zottola, M. A.; Davis, M. W.; Williams, J.; Tuthill, P. A. Peptidyl α -ketoheterocyclic inhibitors of human neutrophil elastase. 3. In vitro and in vivo potency of a series of peptidyl α -ketobenzoxazoles. *J. Med. Chem.* **1995**, *38*, 3972–3982.
- (30) (a) Akiyama, Y.; Tsutsumi, S.; Hatsushiba, E.; Ohuchi, S.; Okonogi, T. Peptidyl α -keto thiazole as potent thrombin inhibitors. *Bioorg. Med. Chem. Lett.* **1997**, *7*, 533–538. (b) Tamura, S. Y.; Shamblin, B. M.; Brunck, T. K.; Ripka, W. C. Rational design, synthesis and serine protease inhibitory activity of novel P₁-argininoyl heterocycles. *Bioorg. Med. Chem. Lett.* **1997**, *7*, 1359–1364. (c) Boatman, P. D.; Ogbu, C. O.; Eguchi, M.; Kim, H.-O.; Nakanishi, H.; Cao, B.; Shea, J. P.; Kahn, M. Secondary structure peptide mimetics: design, synthesis, and evaluation of β -strand mimetic thrombin inhibitors. *J. Med. Chem.* **1999**, *42*, 1367–1375. (d) St. Denis, Y.; Augelli-Szafran, C. E.; Bachand, B.; Berryman, K. A.; DiMaio, J.; Doherty, A. M.; Edmunds, J. J.; Leblond, L.; Levesque, S.; Narasimhan, L. S.; Penvose-Yi, J. R.; Rubin, J. R.; Tarazi, M.; Winocour, P. D.; Siddiqui, M. A. Potent bicyclic lactam inhibitors of thrombin: Part I: P₃ modifications. *Bioorg. Med. Chem. Lett.* **1998**, *8*, 3193–3198. (e) Plummer, J. S.; Berryman, K. A.; Cai, C.; Cody, W. L.; DiMaio, J.; Doherty, A. M.; Edmunds, J. J.; He, J. X.; Holland, D. R.; Levesque, S.; Kent, D. R.; Narasimhan, L. S.; Rubin, J. R.; Rapundalo, S. T.; Siddiqui, M. A.; Susser, A. J.; St-Denis, Y.; Winocour, P. D. Potent and selective bicyclic lactam inhibitors of thrombin: part 2: P₁ modifications. *Bioorg. Med. Chem. Lett.* **1998**, *8*, 3409–3414. (f) Plummer, J. S.; Berryman, K. A.; Cai, C.; Cody, W. L.; DiMaio, J.; Doherty, A. M.; Eaton, S.; Edmunds, J. J.; Holland, D. R.; Lafleur, D.; Levesque, S.; Narasimhan, L. S.; Rubin, J. R.; Rapundalo, S. T.; Siddiqui, M. A.; Susser, A. J.; St. Denis, Y.; Winocour, P. D. Potent and selective bicyclic lactam inhibitors of thrombin: Part 3: P₁' modifications. *Bioorg. Med. Chem. Lett.* **1999**, *9*, 835–840. (g) Leblond, L.; Groulx, B.; Boudreau, C.; Yang, Q.; Siddiqui, M. A.; Winocour, P. D. In vitro and in vivo properties of bicyclic lactam inhibitors. A novel class of low molecular weight peptidomimetic thrombin inhibitors. *Thromb. Res.* **2000**, *100*, 195–209. (h) Narasimhan, L. S.; Rubin, J. R.; Holland, D. R.; Plummer, J. S.; Rapundalo, S. T.; Edmunds, J. E.; St. Denis, Y.; Siddiqui, M. A.; Humblet, C. Structural basis of the thrombin selectivity of a ligand that contains the constrained arginine mimic (2S)-2-amino-(3S)-3-(1-carbamimidoyl-piperidin-3-yl)-propanoic acid at P₁. *J. Med. Chem.* **2000**, *43*, 361–368. (i) Bachand, B.; Tarazi, M.; St. Denis, Y.; Edmunds, J. J.; Winocour, P. D.; Leblond, L.; Siddiqui, M. A. Potent and selective bicyclic lactam inhibitors of thrombin. Part 4: transition state inhibitors. *Bioorg. Med. Chem. Lett.* **2001**, *11*, 287–290. (j) Cody, W. L.; Cai, C.; Doherty, A. M.; Edmunds, J. J.; He, J. X.; Narasimhan, L. S.; Plummer, J. S.; Rapundalo, S. T.; Rubin, J. R.; Van Huis, C. A.; St. Denis, Y.; Winocour, P. D.; Siddiqui, M. A. The design of potent and selective inhibitors of thrombin utilizing a piperazine-dione template. Part 1. *Bioorg. Med. Chem. Lett.* **1999**, *9*, 2497–2502. (k) Cody, W. L.; Augelli-Szafran, C. E.; Berryman, K. A.; Cai, C.; Doherty, A. M.; Edmunds, J. J.; He, J. X.; Narasimhan, L. S.; Penvose-Yi, J.; Plummer, J. S.; Rapundalo, S. T.; Rubin, J. R.; Van Huis, C. A.; Leblond, L.; Winocour, P. D.; Siddiqui, M. A. The design of potent and selective inhibitors of thrombin utilizing a piperazine-dione template: part 2. *Bioorg. Med. Chem. Lett.* **1999**, *9*, 2503–2508. (l) Adang, A. E. P.; de Man, A. P. A.; Vogel, G. M. T.; Grootenhuis, P. D. J.; Smit, M. J.; Peters, C. A. M.; Visser, A.; Rewinkel, J. B. M.; van Dinther, T.; Lucas, H.; Kelder, J.; van Aelst, S.; Meuleman, D. G.; van Boeckel, C. A. A. Unique overlap in the prerequisites for thrombin inhibition and oral bioavailability resulting in potent oral antithrombotics. *J. Med. Chem.* **2002**, *45*, 4419–4432.
- (31) (a) Tsutsumi, S.; Okonogi, T.; Shibahara, S.; Patchett, A. A.; Christensen, B. G. α -Ketothiazole inhibitors of prolyl endopeptidase. *Bioorg. Med. Chem. Lett.* **1994**, *4*, 831–834. (b) Tsutsumi, S.; Okonogi, T.; Shibahara, S.; Ohuchi, S.; Hatsushiba, E.; Patchett, A. A.; Christensen, B. G. Synthesis and structure-activity relationships of peptidyl α -keto heterocycles as novel inhibitors of prolyl endo-peptidase. *J. Med. Chem.* **1994**, *37*, 3492–3502. (c) Ogilvie, W.; Bailey, M.; Poupart, M.-A.; Abraham, A.; Bhavsar, A.; Bonneau, P.; Bordeleau, J.; Bousquet, Y.; Chabot, C.; Duceppe, J.-S.; Fazal, G.; Goulet, S.; Grand-Maitre, C.; Guse, I.; Halmos, T.; Lavallee, P.; Leach, M.; Malenfant, E.; O'Meara, J.; Plante, R.; Plouffe, C.; Poirier, M.; Soucy, F.; Yoakim, C.; Deziel, R. Peptidomimetic inhibitors of the human cytomegalovirus protease. *J. Med. Chem.* **1997**, *40*, 4113–4135. (d) Boger, D. L.; Miyauchi, H.; Hedrick, M. P. α -Keto heterocycle inhibitors of fatty acid amide hydrolase: Carbonyl group modification and α -substitution. *Bioorg. Med. Chem. Lett.* **2001**, *11*, 1517–1520. (e) Zhu, B. Y.; Huang, W.; Su, T.; Marlowe, C.; Sinha, U.; Hollenbach, S.; Scarborough, R. M. Discovery of transition state factor Xa inhibitors as potential anticoagulant agents. *Curr. Top. Med. Chem.* **2001**, *1*, 101–119. (f) Akahoshi, F.; Ashimori, A.; Sakashita, H.; Yoshimura, T.; Imada, T.; Nakajima, M.; Mitsutomi, N.; Kuwahara, S.; Ohtsuka, T.; Fukaya, C.; Miyazaki, M.; Nakamura, N. Synthesis, structure-activity relationships, and pharmacokinetic profiles of nonpeptidic α -keto heterocycles as novel inhibitors of human chymase. *J. Med. Chem.* **2001**, *44*, 1286–1296. (g) Narjes, F.; Koehler, K. F.; Koch, U.; Gerlach, B.; Colarusso, S.; Steinkuhler, C.; Brunetti, M.; Altamura, S.; De Francesco, R.; Matassa, V. G. A designed P₁ cysteine mimetic for covalent and non-covalent inhibitors of HCV NS3 protease. *Bioorg. Med. Chem. Lett.* **2002**, *12*, 701–704. (h) South, M. S.; Case, B. L.; Wood, R. S.; Jones, D. E.; Hayes, M. J.; Girard, T. J.; Lachance, R. M.; Nicholson, N. S.; Clare, M.; Stevens, A. M.; Stegeman, R. A.; Stallings, W. C.; Kyrumbaail, R. G.; Parlow, J. J. Structure-based drug design of pyrazinone antithrombotics as selective inhibitors of the tissue factor VIIa complex. *Bioorg. Med. Chem. Lett.* **2003**, *13*, 2319–2325.
- (32) (a) Tao, M.; Bihovsky, R.; Kauer, J. C. Inhibition of calpain by peptidyl heterocycles. *Bioorg. Med. Chem. Lett.* **1996**, *6*, 3009–3012. (b) Dragovich, P. S.; Zhou, R.; Webber, S. E.; Prins, T. J.; Kwok, A. K.; Okano, K.; Fuhrman, S. A.; Zalman, L. S.; Maldonado, F. C.; Brown, E. L.; Meador, J. W., III; Patick, A. K.; Ford, C. E.; Brothers, M. A.; Binford, S. L.; Matthews, D. A.; Ferre, R. A.; Worland, S. T. Structure-based design of ketone-containing, tripeptidyl human rhinovirus 3C protease inhibitors. *Bioorg. Med. Chem. Lett.* **2000**, *10*, 45–48.
- (33) (a) Abbreviations: Cbz, carbobenzoxy; DCC, dicyclohexylcarbodiimide; HOBt, 1-hydroxybenzotriazole; TFA, trifluoroacetic acid; TMS, trimethylsilyl; Ts, *p*-toluenesulfonyl. (b) Reference to the Dess–Martin oxidation: Dess, D. B.; Martin, J. C. A useful 12-*I*-5 triacetoxypiperidine (the Dess–Martin piperidine) for the selective oxidation of primary or secondary alcohols and a variety of related 12-*I*-5 species. *J. Am. Chem. Soc.* **1991**, *113*, 7277–7287. (c) The crude target compounds from both synthetic routes generally contained 10–20% of the epimeric D-Arg tripeptide (confirmed by independent synthesis for selected analogues), most of which was removed during purification by reverse-phase HPLC. The L/D-Arg diastereomeric ratios were usually determined in many cases either by analytical HPLC or by proton NMR integration of the *N*-methyl or Arg α -methine signals.²⁵ (d) The proton on the stereogenic center adjacent to the activated ketone is labile such that stereomutation can take place during synthetic processes, biochemical assays, or in vivo experiments. For this reason, the ketone is not generated until the end of a synthetic sequence, and HPLC separations are performed with some trifluoroacetic acid present. To understand this stereomutation and to establish suitable conditions for the in vitro bioassays, we conducted some epimerization studies.²⁵ For example, with benzothiazole **6b** (L-Arg/D-Arg = 98:2) in a pH

- 7.4 buffer (that used for the thrombin inhibition assay) at 37 °C, the L-Arg/D-Arg isomer ratio changed to 70:30 after 0.5 h, 60:40 after 1 h, and 50:50 after 6.5 h. In general, the compounds are fairly stable stereochemically at pH 2–6.5, and they are stable when stored as acid-addition salts. To probe in vivo epimerization, we examined **6a** in rat plasma at pH 7.4. At 23 °C the amount of D-Arg isomer increased over 2 h from 5% to 40%; at 37 °C, a L-Arg/D-Arg ratio of 57:43 was reached after just 1 h.
- (34) Also, a comparison of **7e** with **7f** and **7g** shows a 20-fold to 25-fold loss in potency by removing the benzo group.
- (35) The carboxylate also hydrogen-bonds with a water molecule and forms a salt bridge with the amino groups of Lys-236 and Lys-240.^{25,27b}
- (36) Chan, A. W. E.; Golec, J. M. C. Prediction of relative potency of ketone protease inhibitors using molecular orbital theory. *Bioorg. Med. Chem.* **1996**, *4*, 1673–1677. Abbotta, A.; Bradamante, S.; Pagani, G. A. Diheteroarylmethanes. 5. *E-Z* Isomerism of carbanions substituted by 1,3-azoles: ¹³C and ¹⁵N π charge/shift relationships as a source for mapping charge and ranking the electron-withdrawing power of heterocycles. *J. Org. Chem.* **1996**, *61*, 1761–1769.
- (37) Sorbera, L. A.; Bayes, M.; Castaner, J.; Silvestre, J. Melagatran and ximelagatran: anticoagulant thrombin inhibitor. *Drugs Future* **2001**, *26*, 1155–1170. Gustafsson, D.; Nystrom, J.-E.; Carlsson, S.; Bredberg, U.; Eriksson, U.; Gyzander, E.; Elg, M.; Antonsson, T.; Hoffmann, K.-J.; Ungell, A.-L.; Sorensen, H.; Nagard, S.; Abrahamsson, A.; Bylund, R. The direct thrombin inhibitor melagatran and its oral prodrug H 376/95: Intestinal absorption properties, biochemical and pharmacodynamic effects. *Thromb. Res.* **2001**, *101*, 171–181. Sarich, T. C.; Eriksson, U. G.; Mattsson, C.; Wolzt, M.; Frison, L.; Fager, G.; Gustafsson, D. Inhibition of thrombin generation by the oral direct thrombin inhibitor ximelagatran in shed blood from healthy male subjects. *Thromb. Haemostasis* **2002**, *87*, 300–305. Hopfner, R. Ximelagatran (AstraZeneca). *Curr. Opin. Invest. Drugs* **2002**, *3*, 246–251.
- (38) Recacha, R.; Carson, M.; Costanzo, M. J.; Maryanoff, B.; DeLucas, L. J.; Chattopadhyay, D. Structure of the RWJ-51084-bovine pancreatic β -trypsin complex at 1.8 Å. *Acta Crystallogr.* **1999**, *D55*, 1785–1791.
- (39) Derian, C. K.; Maryanoff, B. E.; Zhang, H.-C.; Andrade-Gordon, P. Design and evaluation of potent peptide-mimetic PAR-1 antagonists. *Drug Dev. Res.* **2003**, *59*, 355–366. Maryanoff, B. E.; Zhang, H.-C.; Andrade-Gordon, P.; Derian, C. K. Discovery of potent peptide-mimetic antagonists for the human thrombin receptor, protease-activated receptor 1 (PAR-1). *Curr. Med. Chem.: Cardiovasc. Hematol. Agents* **2003**, *1*, 13–36. Derian, C. K.; Maryanoff, B. E.; Zhang, H.-C.; Andrade-Gordon, P. Therapeutic potential of protease-activated receptor-1 antagonists. *Expert Opin. Invest. Drugs* **2003**, *12*, 209–221. Maryanoff, B. E.; Santulli, R.; McComsey, D. F.; Zhang, H.-C.; Hoekstra, W. J.; Hoey, K.; Smith, C. E.; Addo, M. F.; Darrow, A. L.; Andrade-Gordon, P. Protease-activated receptor-2 (PAR-2): structure-function study of receptor activation by diverse peptides related to tethered-ligand epitopes. *Arch. Biochem. Biophys.* **2001**, *386*, 195–204.
- (40) Costanzo, M. J.; Yabut, S. C.; Almond, H. R., Jr.; Andrade-Gordon, P.; Corcoran, T. W.; de Garavilla, L.; Kauffman, J. A.; Abraham, W. M.; Recacha, R.; Chattopadhyay, D.; Maryanoff, B. E. Potent, small-molecule inhibitors of human mast cell tryptase. Anti-asthmatic action of a dipeptide-based transition-state analogue containing a benzothiazole ketone. *J. Med. Chem.* **2003**, *46*, 3865–3876.
- (41) Caughey, G. H. *Mast Cell Proteases in Immunology and Biology*; Marcel Dekker: New York, 1995. Caughey, G. H. Of mites and men: trypsin-like proteases in the lungs. *Am. J. Respir. Cell Mol. Biol.* **1997**, *16*, 621–628. Schwartz, L. B. Mast cell tryptase: properties and roles in human allergic responses. *Clin. Allergy Immunol.* **1995**, *6*, 9–23. Schwartz, L. B. Tryptase: a mast cell serine protease. *Methods Enzymol.* **1994**, *244*, 88–100. Schwartz, L. B.; Lewis, R. A.; Austen, K. F. Tryptase from human pulmonary mast cells. Purification and characterization. *J. Biol. Chem.* **1981**, *256*, 11939–11943.
- (42) Pereira, P. J. B.; Bergner, A.; Macedo-Ribeiro, S.; Huber, R.; Matschiner, G.; Fritz, H.; Sommerhoff, C. P.; Bode, W. Human β -tryptase is a ring-like tetramer with active sites facing a central pore. *Nature (London)* **1998**, *392*, 306–311.
- (43) (a) Molinari, J. F.; Scuri, M.; Moore, W. R.; Clark, J.; Tanaka, R.; Abraham, W. M. Inhaled tryptase causes bronchoconstriction in sheep via histamine release. *Am. J. Respir. Crit. Care Med.* **1996**, *154*, 649–653. (b) Clark, J.; Abraham, W. M.; Fishman, C. E.; Forteza, R.; Ahmed, A.; Cortes, A.; Warne, R. L.; Moore, W. R.; Tanaka, R. D. Tryptase inhibitors block allergen-induced airway and inflammatory responses in allergic sheep. *Am. J. Respir. Crit. Care Med.* **1995**, *152*, 2076–2083.
- (44) For reviews on tryptase inhibitors, see the following. Clark, J. M.; Moore, W. R.; Tanaka, R. D. Tryptase inhibitors: a new class of antiinflammatory drugs. *Drugs Future* **1996**, *21*, 811–816. (Update: Anonymous. APC-366. *Drugs Future* **1998**, *23*, 903.) Rice, K. D.; Tanaka, R. D.; Katz, B. A.; Numerof, R. P.; Moore, W. R. Inhibitors of tryptase for the treatment of mast-cell-mediated diseases. *Curr. Pharm. Des.* **1998**, *4*, 381–396. Burgess, L. E. Mast cell tryptase as a target for drug design. *Drug News Perspect.* **2000**, *13*, 147–156.
- (45) A single-crystal X-ray analysis of the sulfate salt of **10** confirmed the (2*S*)-stereochemistry.⁴⁰
- (46) Bainton, D. F.; Ullyot, J. L.; Farquhar, M. G. The development of neutrophilic polymorphonuclear leukocytes in human bone marrow. *J. Exp. Med.* **1971**, *134*, 907–934. Baggiolini, M.; Bretz, U.; Dewald, B.; Feigenson, M. E. The polymorphonuclear leukocyte. *Agents Actions* **1978**, *8*, 3–10. Hanson, R. K.; Connolly, N. L.; Burnett, D.; Campbell, E. J.; Senior, R. M.; Ley, T. J. Developmental regulation of the human cathepsin G gene in myelomonocytic cells. *J. Biol. Chem.* **1990**, *265*, 1524–1530. Owen, C. A.; Campbell, E. J. The cell biology of leukocyte-mediated proteolysis. *J. Leukocyte Biol.* **1999**, *65*, 137–150.
- (47) (a) Groutas, W. C. Inhibitors of leukocyte elastase and leukocyte cathepsin G. Agents for the treatment of emphysema and related ailments. *Med. Res. Rev.* **1987**, *7*, 227–241. (b) Lomas, D. A.; Stone, S. R.; Llewellyn-Jones, C.; Keogan, M.-T.; Wang, Z.; Rubin, H.; Carrell, R. W.; Stockley, R. A. The control of neutrophil chemotaxis by inhibitors of cathepsin G and chymotrypsin. *J. Biol. Chem.* **1995**, *270*, 23437–23443. (c) Groutas, W. C.; Kuang, R.; Venkataraman, R.; Epp, J. B.; Ruan, S.; Prakash, O. Structure-based design of a general class of mechanism-based inhibitors of the serine proteinases employing a novel amino acid-derived heterocyclic scaffold. *Biochemistry* **1997**, *36*, 4739–4750. (d) Gütschow, M.; Neumann, U. Inhibition of cathepsin G by 4H-3,1-benzoxazin-4-ones. *Bioorg. Med. Chem.* **1997**, *5*, 1935–1942. (e) Kuang, R.; Epp, J. B.; Ruan, S.; Yu, H.; Huang, P.; He, S.; Tu, J.; Schechter, N. M.; Turbov, J.; Froelich, C. J.; Groutas, W. C. A general inhibitor scaffold for serine proteases with a (chymo)trypsin-like fold: solution-phase construction and evaluation of the first series of libraries of mechanism-based inhibitors. *J. Am. Chem. Soc.* **1999**, *121*, 8128–8129. (f) MacIvor, D. M.; Shapiro, S. D.; Pham, C. T. N.; Belaaouaj, A.; Abraham, S. N.; Ley, T. J. Normal neutrophil function in cathepsin G-deficient mice. *Blood* **1999**, *94*, 4282–4293. (g) Owen, C. A.; Campbell, E. J. Neutrophil proteinases and matrix degradation. The cell biology of pericellular proteolysis. *Semin. Cell Biol.* **1995**, *6*, 367–376.
- (48) Roughley, P. J.; Barrett, A. J. The degradation of cartilage proteoglycans by tissue proteinases. Proteoglycan structure and its susceptibility to proteolysis. *Biochem. J.* **1977**, *167*, 629–637. Capodici, C.; Berg, R. A. Cathepsin G degrades denatured collagen. *Inflammation* **1989**, *13*, 137–145. Vartio, T.; Seppa, H.; Vaheri, A. Susceptibility of soluble and matrix fibronectins to degradation by tissue proteinases, mast cell chymase and cathepsin G. *J. Biol. Chem.* **1981**, *256*, 471–477. Reilly, C. F.; Travis, J. The degradation of human lung elastin by neutrophil proteinases. *Biochim. Biophys. Acta* **1980**, *621*, 147–157.
- (49) Sambrano, G. R.; Huang, W.; Faruqi, T.; Mahrus, S.; Craik, C.; Coughlin, S. R. Cathepsin G activates protease-activated receptor-4 in human platelets. *J. Biol. Chem.* **2000**, *275*, 6819–6823. Wu, C.-C.; Hwang, T.-L.; Liao, C.-H.; Kuo, S.-C.; Lee, F.-Y.; Lee, C.-Y.; Teng, C.-M. Selective inhibition of protease-activated receptor 4-dependent platelet activation by YD-3. *Thromb. Haemostasis* **2002**, *8*, 1026–1033.
- (50) (a) Groutas, W. C.; Kuang, R.; Ruan, S.; Epp, J. B.; Venkataraman, R.; Truong, T. M. Potent and specific inhibition of human leukocyte elastase, cathepsin G and proteinase 3 by sulfone derivatives employing the 1,2,5-thiadiazolidin-3-one 1,1-dioxide scaffold. *Bioorg. Med. Chem.* **1998**, *6*, 661–671. (b) Iijima, K.; Katada, J.; Yasadu, E.; Uno, I.; Hayashi, Y. *N*-[2,2-Dimethyl-3-(*N*-(4-cyanobenzoyl)amino)-nonanoyl]-*L*-phenylalanine ethyl ester as a stable ester-type inhibitor of chymotrypsin-like serine proteases: structural requirements for potent inhibition of α -chymotrypsin. *J. Med. Chem.* **1999**, *42*, 312–323. (c) Powers, J. C.; Tanaka, T.; Harper, J. W.; Minematsu, Y.; Baker, L.; Lincoln, D.; Crumley, K. V. Mammalian chymotrypsin-like enzymes. Comparative reactivities of rat mast cell proteases, human and dog skin chymases, and human cathepsin G with peptide 4-nitroanilide substrates and with peptide chloromethyl ketone and sulfonyl fluoride inhibitors. *Biochemistry* **1985**, *24*, 2048–2058. (d) Harper, J. W.; Powers, J. C. Reaction of serine proteases with substituted 3-alkoxy-4-chloroisocoumarins and 3-alkoxy-7-amino-4-chloroisocoumarins: new reactive mechanism-based inhibitors. *Biochemistry* **1985**, *24*, 7200–7213 and references therein. (e) Peet, N. P.; Burkhardt, J. P.; Angelastro, M. R.; Giroux, E. L.; Mehdi, S.; Bey, P.; Kolb, M.; Neises, B.; Schirlin, D. Synthesis of peptidyl fluoromethyl ketones and peptidyl α -keto esters as inhibitors of porcine pancreatic elastase, human neutrophil elastase, and rat and human neutrophil

- cathepsin G. *J. Med. Chem.* **1990**, *33*, 394–407. (f) Groutas, W. C.; Brubaker, M. J.; Venkataraman, R.; Epp, J. B.; Stanga, M. A.; McClenahan, J. J. Inhibitors of human neutrophil cathepsin G: structural and biochemical studies. *Arch. Biochim. Biophys.* **1992**, *294*, 144–146. (g) Knight, W. B.; Chabin, R.; Green, B. Inhibition of human serine proteases by substituted 2-azetidionones. *Arch. Biochim. Biophys.* **1992**, *296*, 704–708. (h) Zembower, D. E.; Kam, C.-M.; Powers, J. C.; Zalkow, L. H. Novel anthraquinone inhibitors of human leukocyte elastase and cathepsin G. *J. Med. Chem.* **1992**, *35*, 1597–1605.
- (51) Hof, P.; Mayr, I.; Huber, R.; Korzus, E.; Potempa, J.; Travis, J.; Powers, J. C.; Bode, W. The 1.8 Å crystal structure of human cathepsin G in complex with Suc-Val-Pro-PheP-(OPh)₂: a Janus-faced proteinase with two opposite specificities. *EMBO J.* **1996**, *15*, 5481–5491.
- (52) Greco, M. N.; Hawkins, M. J.; Powell, E. T.; Almond, H. R., Jr.; Corcoran, T. W.; de Garavilla, L.; Kauffman, J. A.; Recacha, R.; Chattopadhyay, D.; Andrade-Gordon, P.; Maryanoff, B. E. Non-peptide inhibitors of cathepsin G: optimization of a novel β-ketophosphonic acid lead by structure-based drug design. *J. Am. Chem. Soc.* **2002**, *124*, 3810–3811.
- (53) The O_γ of Ser-195 is proximal to this oxygen atom on the phosphorus (distance of 3.3 Å) and may be involved in a hydrogen bond.
- (54) We were limited to using secondary amines because use of a primary amine in the DCC coupling gave an undesired phthalimide product and little of the desired NH amide (Scheme 4).
- (55) Greco, M. N.; Almond, H. R., Jr.; de Garavilla, L.; Hawkins, M. J.; Maryanoff, B. E.; Qian, Y.; Walker, D. G.; Cesco-Cancian, S.; Nilsen, C. N.; Patel, M. N.; Humora, M. J. Preparation of novel phosphonic acid compounds as inhibitors of serine proteases. PCT Int. Patent Appl. WO 0335654, 2003.
- (56) (a) Caughey, G. H. Serine proteinases of mast cell and leukocyte granules. A league of their own. *Am. J. Resp. Crit. Care Med.* **1994**, *150*, S138–S142. (b) Caughey, G. H. New developments in the genetics and activation of mast cell proteases. *Mol. Immunol.* **2002**, *38*, 1353–1357. (c) Schechter, N. M.; Pereira, P. J. B.; Strobl, S. Structure and function of human chymase. In *Mast Cells and Basophils*; Marone, G., Lichtenstein, L. M., Galli, S. J., Eds.; Academic Press: San Diego, CA, 2000; pp 275–290. (d) Takai, S.; Miyazaki, M. The role of chymase in vascular proliferation. *Drug News Perspect.* **2002**, *15*, 278–282. (e) Miller, H. R. P.; Pemberton, A. D. Tissue-specific expression of mast cell granule serine proteinases and their role in inflammation in the lung and gut. *Immunology* **2002**, *105*, 375–390. (f) Walls, A. F. Mast cell proteases in asthma. *Lung Biol. Health Dis.* **1998**, *117*, 89–110. (g) Welle, M. Development, significance, and heterogeneity of mast cells with particular regard to the mast cell-specific proteases chymase and tryptase. *J. Leukocyte Biol.* **1997**, *61*, 233–245. (h) Dell'Italia, L. J.; Husain, A. Dissecting the role of chymase in angiotensin II formation and heart and blood vessel diseases. *Curr. Opin. Cardiol.* **2002**, *17*, 374–379.
- (57) (a) Akahoshi, F. Chymase inhibitors and their therapeutic potential. *Drugs Future* **2002**, *27*, 765–770. (b) Akahoshi, F. Nonpeptidic chymase inhibitors: design and structure–activity relationships of pyrimidinone derivatives based on the predicted binding mode of a peptidic inhibitor. *Curr. Pharm. Des.* **2003**, *9*, 1191–1199. (c) Aoyama, Y. Non-peptidic chymase inhibitors. *Expert Opin. Ther. Pat.* **2001**, *11*, 1423–1428. (d) Doggrell, S. A.; Wanstall, J. C. Will chymase inhibitors be the next major development for the treatment of cardiovascular disorders? *Expert Opin. Invest. Drugs* **2003**, *12*, 1429–1432. (e) Fukami, H.; Okunishi, H.; Miyazaki, M. Chymase: its pathophysiological roles and inhibitors. *Curr. Pharm. Des.* **1998**, *4*, 439–453.
- (58) (a) Given the two crystal structures of human chymase complexed with inhibitors, structure-based drug design is applicable to this target.^{58b} (b) McGrath, M. E.; Mirzadegan, T.; Schmidt, B. F. Crystal structure of phenylmethanesulfonyl fluoride-treated human chymase at 1.9 Å. *Biochemistry* **1997**, *36*, 14318–14324. Pereira, P. J. B.; Wang, Z.-M.; Rubin, H.; Huber, R.; Bode, W.; Schechter, N. M.; Strobl, S. The 2.2 Å crystal structure of human chymase in complex with succinyl-Ala-Ala-Pro-Phe-chloromethylketone: structural explanation for its dipeptidyl carboxypeptidase specificity. *J. Mol. Biol.* **1999**, *286*, 163–173.
- (59) Details on pharmacological studies and specific compounds will be disclosed in a separate publication at a later date. Some pertinent information is contained in our published patent application.⁵⁵
- (60) For reviews, see the following. (a) Oleksyszyn, J.; Powers, J. C. Amino acid and peptide phosphonate derivatives as specific inhibitors of serine peptidases. *Methods Enzymol.* **1994**, *244*, 423–441. (b) Collinsova, M.; Jiracek, J. Phosphonic acid compounds in biochemistry, biology and medicine. *Curr. Med. Chem.* **2000**, *7*, 629–647.
- (61) (a) Cheng, L.; Goodwin, C. A.; Scully, M. F.; Kakkar, V. V.; Claeson, G. Substrate-related phosphonopeptides, a new class of thrombin inhibitors. *Tetrahedron Lett.* **1991**, *32*, 7333–7336. (b) Wang, C.-L.; Taylor, T. L.; Mical, A. J.; Spitz, S.; Reilly, T. M. Synthesis of phosphonopeptides as thrombin inhibitors. *Tetrahedron Lett.* **1992**, *33*, 7667–7670. (c) Fastrez, J.; Jespers, L.; Lison, D.; Renard, M.; Sonveaux, E. Synthesis of new phosphonate inhibitors of serine proteases. *Tetrahedron Lett.* **1989**, *30*, 6861–6864. (d) Bartlett, P. A.; Lamden, L. A. Inhibition of chymotrypsin by phosphonate and phosphoramidate peptide analogs. *Bioorg. Chem.* **1986**, *14*, 356–377. (e) Bertrand, J. A.; Oleksyszyn, J.; Kam, C.-M.; Boduszek, B.; Presnell, S.; Plaskon, R. R.; Suddath, F. L.; Powers, J. C.; Williams, L. D. Inhibition of trypsin and thrombin by amino(4-amidinophenyl)-methanephosphonate diphenyl ester derivatives: X-ray structures and molecular models. *Biochemistry* **1996**, *35*, 3147–3155. (f) Oleksyszyn, J.; Powers, J. C. Irreversible inhibition of serine proteases by peptide derivatives of (α-aminoalkyl)phosphonate diphenyl esters. *Biochemistry* **1991**, *30*, 485–493. (g) Bone, R.; Sampson, N. S.; Bartlett, P. A.; Agard, D. A. Crystal structures of α-lytic protease complexes with irreversibly bound phosphonate esters. *Biochemistry* **1991**, *30*, 2263–2272. (h) Sampson, N. S.; Bartlett, P. A. Peptidic phosphorylating agents as irreversible inhibitors of serine proteases and models of the tetrahedral intermediates. *Biochemistry* **1991**, *30*, 2255–2263.
- (62) Note: There is a reference numbering error in the text of this section in our *J. Am. Chem. Soc.* paper;⁵² footnote “5a” should actually be “4a”.
- (63) Li, M.; Lin, Z.; Johnson, M. E. Structure-based design and synthesis of novel thrombin inhibitors based on phosphonic peptide mimetics. *Bioorg. Med. Chem. Lett.* **1999**, *9*, 1957–1962.

JM030493T